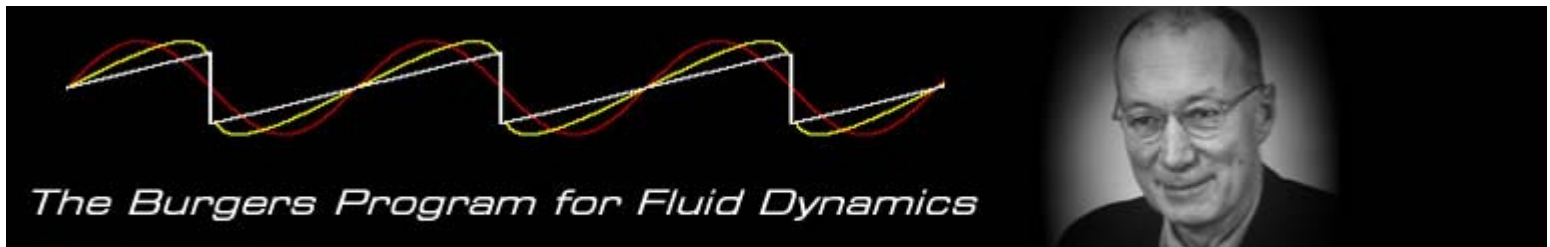




Twenty Years of **Experimental** and **DNS** Access
to the **Velocity Gradient Tensor**: What Have We
Learned About Turbulence?

James M. Wallace



 UNIVERSITY OF
MARYLAND

Background & Overview



*“...vorticity measurements suggest themselves as the most promising method for a quantitative study of ordered motion. ...unfortunately...direct measurement of vorticity has not yet been successfully accomplished with sufficient accuracy.” (Laufer, *Ann. Rev. Fl. Mech.* 7, 1975).*

As recently as twenty years ago there was still no experimental or computational access to the **velocity gradient tensor** for turbulent flows. Vorticity, dissipation and strain rates and helicity, were inaccessible.

In 1987 **measurements** of all the components of the velocity gradient tensor in a turbulent boundary layer by a **multi-sensor hot-wire probe** were published (*Balint, Vukoslavčević & Wallace, Advances in Turbulence, Proc. 1st Euro. Turb. Conf.*)

In 1987 the first **DNS** of homogeneous turbulent shear flow (*Rogers & Moin, JFM 176* and *Ashurt, Kerstein, Kerr & Gibson and, Phys. Fluids 30*) and of a turbulent channel flow (*Kim, Moin & Moser, JFM 177*) were successfully completed and reported.

PIV with sufficient spatial resolution was developed in the 1990's to provide another means of access to these fundamental properties of turbulence.

This presentation will review these remarkable developments and point out some of the most important things we have learned about turbulence as a result.

Acknowledgements



Co-workers:

Elias Balaras
Jean-Louis Balint
Peter Bernard
Lawrence Ong
Ugo Piomelli
Serge Simöens
Petar Vukoslavčević

Students:

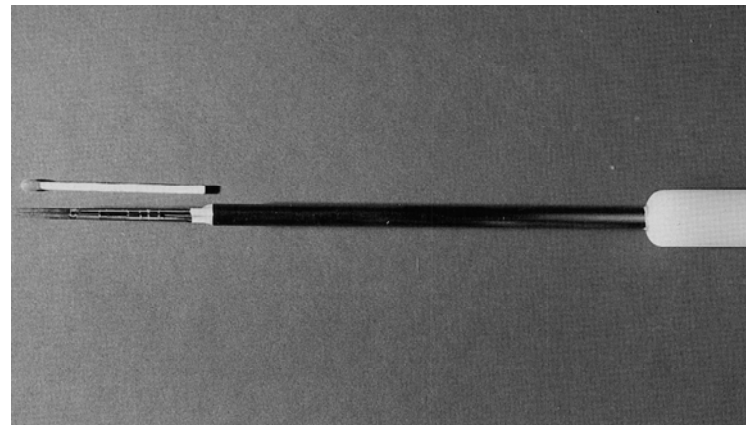
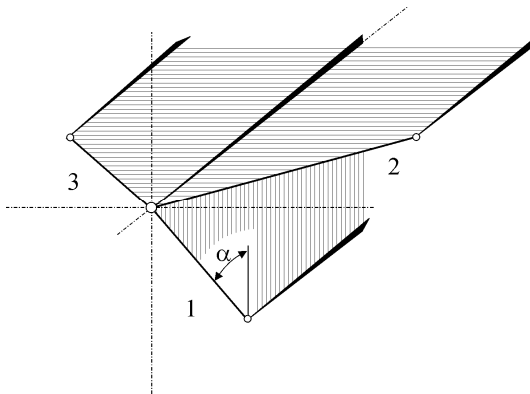
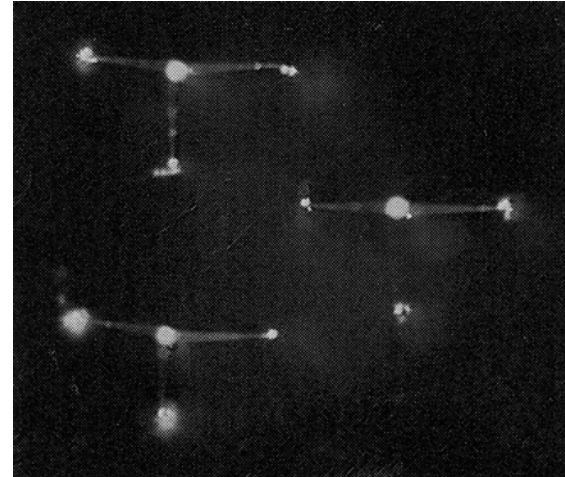
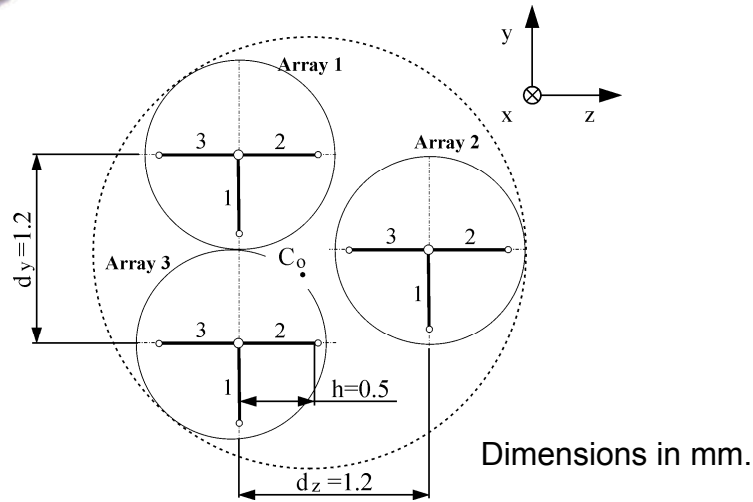
Alan Folz
Eleftharis Kastrinakis
Rick Loucks
Ning Li
Seong-Ryong Park
Phuc Nguyen
Bill Wassmann

Colleagues:

Yannis Andreopoulos
Ron Adrian
Bob Brodkey
Jim Duncan
Helmut Eckelmann
John Foss
Fazle Hussain
Ken Kiger
John Kim
Parviz Moin
Bob Moser
Ron Panton
Mike Rogers
Phillipe Spalart
Arkady Tsinober

Support over the years by:
NSF, DOE, NASA, CTR summer program

Nine-Sensor Hot-wire Probe

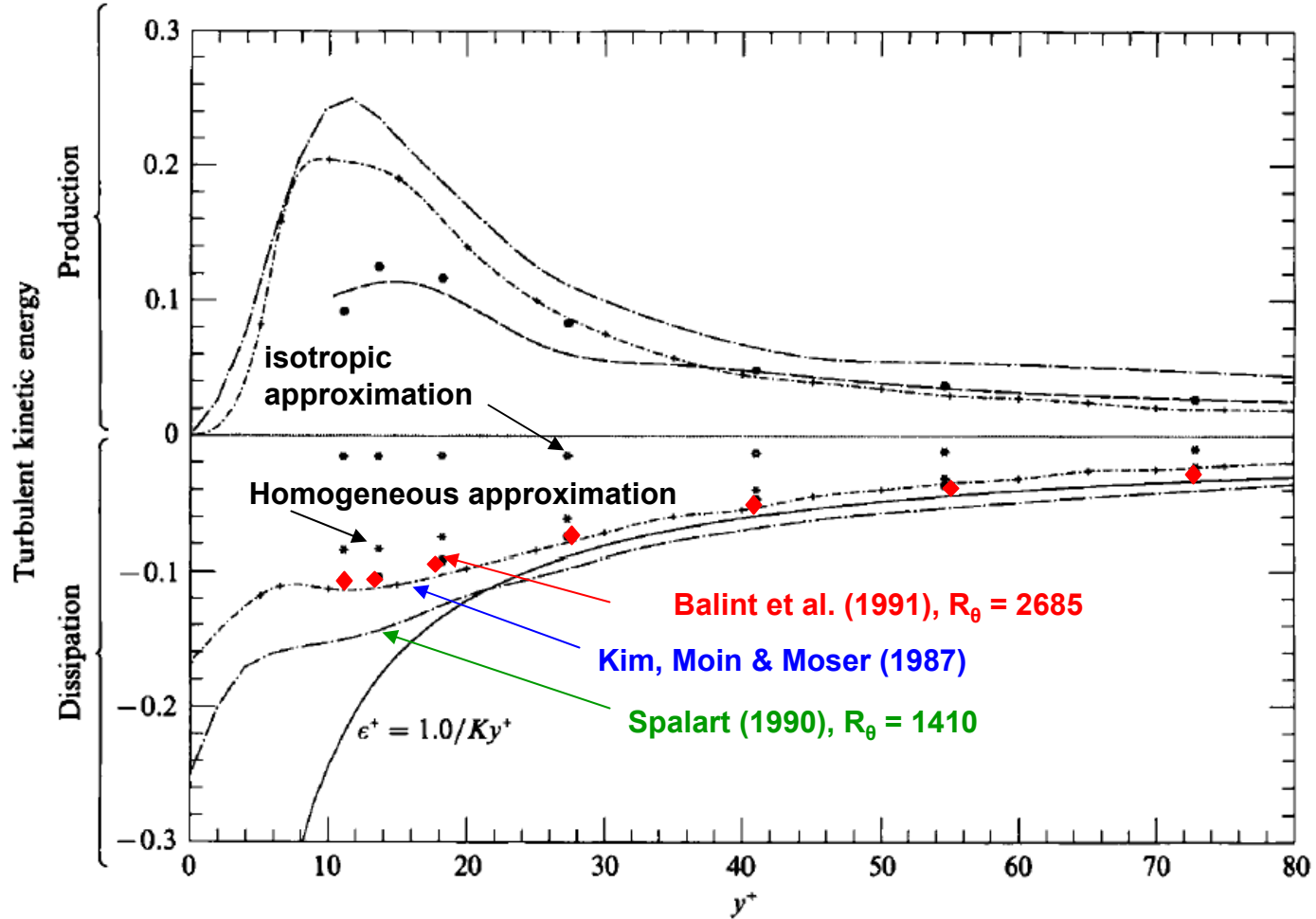


Vukoslavčević, Balint & Wallace. (1991)

JFM 228



Turbulent Kinetic Energy Production & Dissipation Rate in a Turbulent Boundary Layer

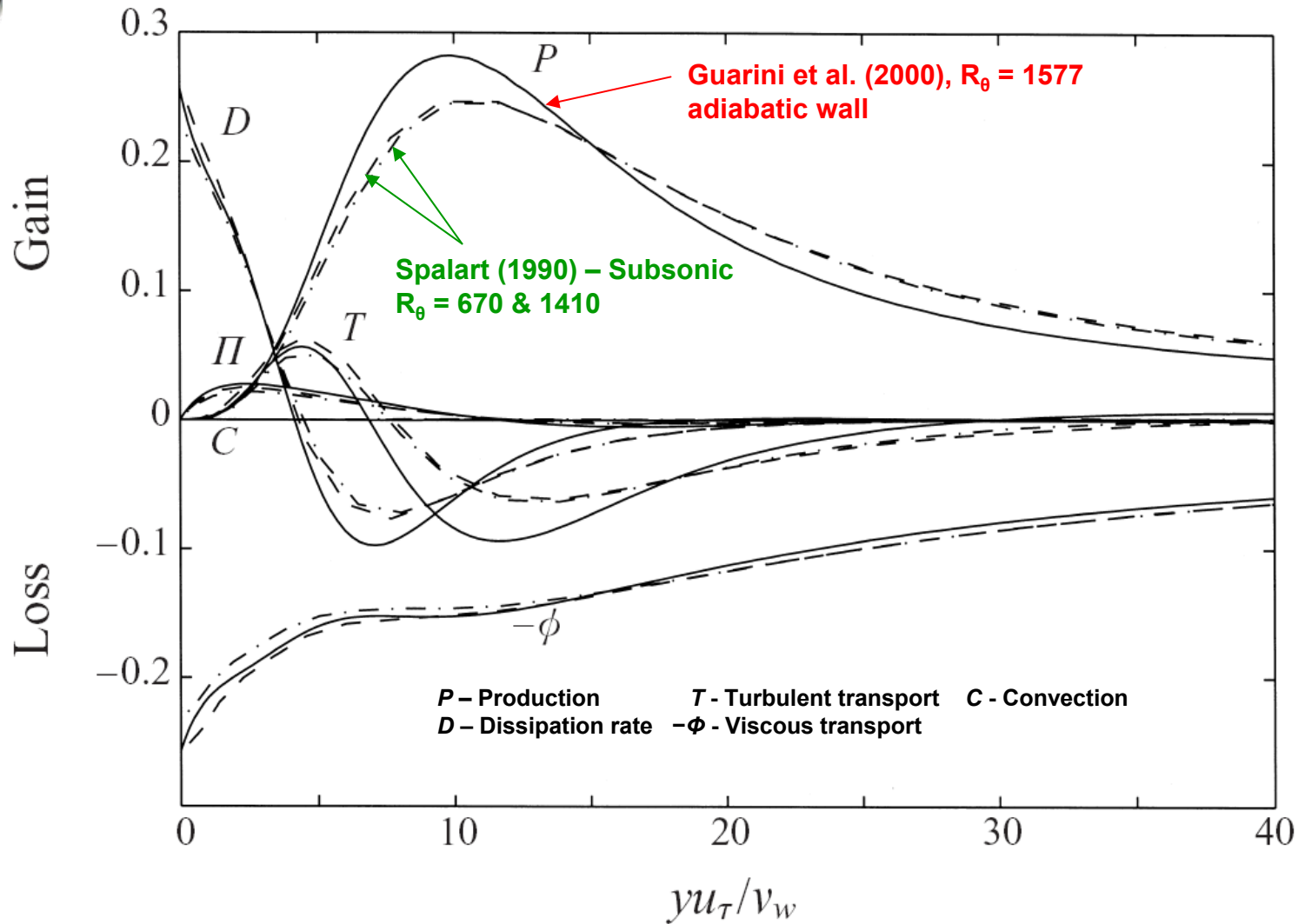


Balint, Vukoslavčević & Wallace. (1991)

JFM 228



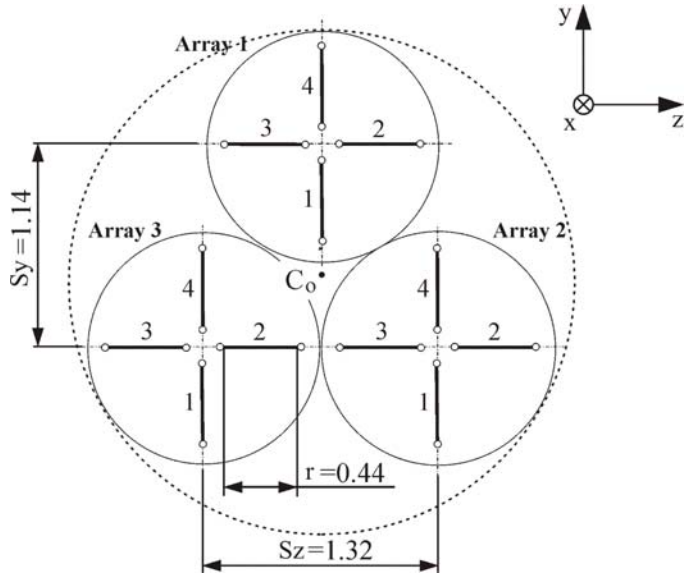
DNS Turbulent Kinetic Energy Budget in a Supersonic Boundary Layer at Mach 2.5



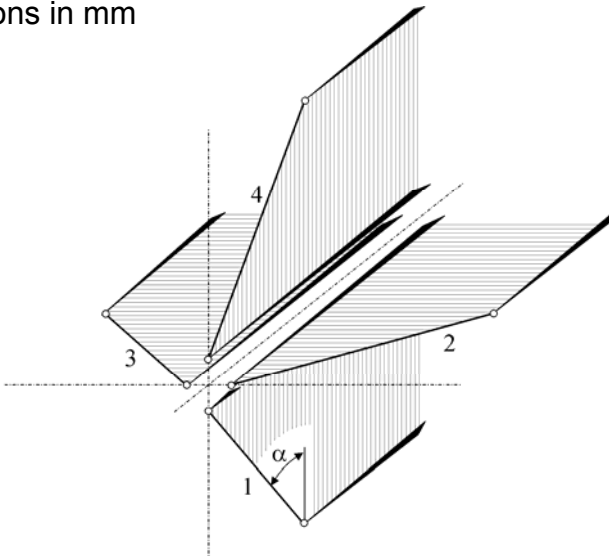
S. E. Guarini, R. D. Moser, K. Shariff & A. Wray (2000)

JFM 414

12-Sensor Hot-Wire Probe



Dimensions in mm



12-sensor Probe Data Processing



Taylor's series expansion of velocity components about probe cross-stream plane centroid to center of the jth sensor over the measured distances, C_j and D_j .

$$U_{1j} = U_{1o} + C_j \frac{\partial U_1}{\partial y} + D_j \frac{\partial U_1}{\partial z}$$

$$U_{2j} = U_{2o} + C_j \frac{\partial U_2}{\partial y} + D_j \frac{\partial U_2}{\partial z}$$

$$U_{3j} = U_{3o} + C_j \frac{\partial U_3}{\partial y} + D_j \frac{\partial U_3}{\partial z}$$

12 Cooling equations for each of the j sensors in terms of the three velocity components at the probe centroid and the six velocity gradients in the cross-stream plane.

$$f_j \equiv - [P_j] + U_{1o}^2 + 2C_j U_{1o} \frac{\partial U_1}{\partial y} + 2D_j U_{1o} \frac{\partial U_1}{\partial z}$$

$$- k_{2j} \left[U_{2o}^2 + 2C_j U_{2o} \frac{\partial U_2}{\partial y} + 2D_j U_{2o} \frac{\partial U_2}{\partial z} \right]$$

$$- k_{3j} \left[U_{3o}^2 + 2C_j U_{3o} \frac{\partial U_3}{\partial y} + 2D_j U_{3o} \frac{\partial U_3}{\partial z} \right]$$

$$- k_{4j} \left[U_{1o} U_{2o} + C_j \left(U_{1o} \frac{\partial U_2}{\partial y} + U_{2o} \frac{\partial U_1}{\partial y} \right) + D_j \left(U_{1o} \frac{\partial U_2}{\partial z} + U_{2o} \frac{\partial U_1}{\partial z} \right) \right]$$

$$- k_{5j} \left[U_{1o} U_{3o} + C_j \left(U_{1o} \frac{\partial U_3}{\partial y} + U_{3o} \frac{\partial U_1}{\partial y} \right) + D_j \left(U_{1o} \frac{\partial U_3}{\partial z} + U_{3o} \frac{\partial U_1}{\partial z} \right) \right]$$

$$- k_{6j} \left[U_{2o} U_{3o} + C_j \left(U_{2o} \frac{\partial U_3}{\partial y} + U_{3o} \frac{\partial U_2}{\partial y} \right) + D_j \left(U_{2o} \frac{\partial U_3}{\partial z} + U_{3o} \frac{\partial U_2}{\partial z} \right) \right] = 0$$

$$P_j = [A_{1j}] + [A_{2j}] E_j + [A_{3j}] E_j^2 + [A_{4j}] E_j^3 + [A_{5j}] E_j^4$$

is a **polynomial** of the measured voltages, E_j .

120 calibration coefficients, A_{ij} and k_{ij} to be determined .

System of equations solved by minimizing the error function $\sum f_j=0$ iteratively at each time step.



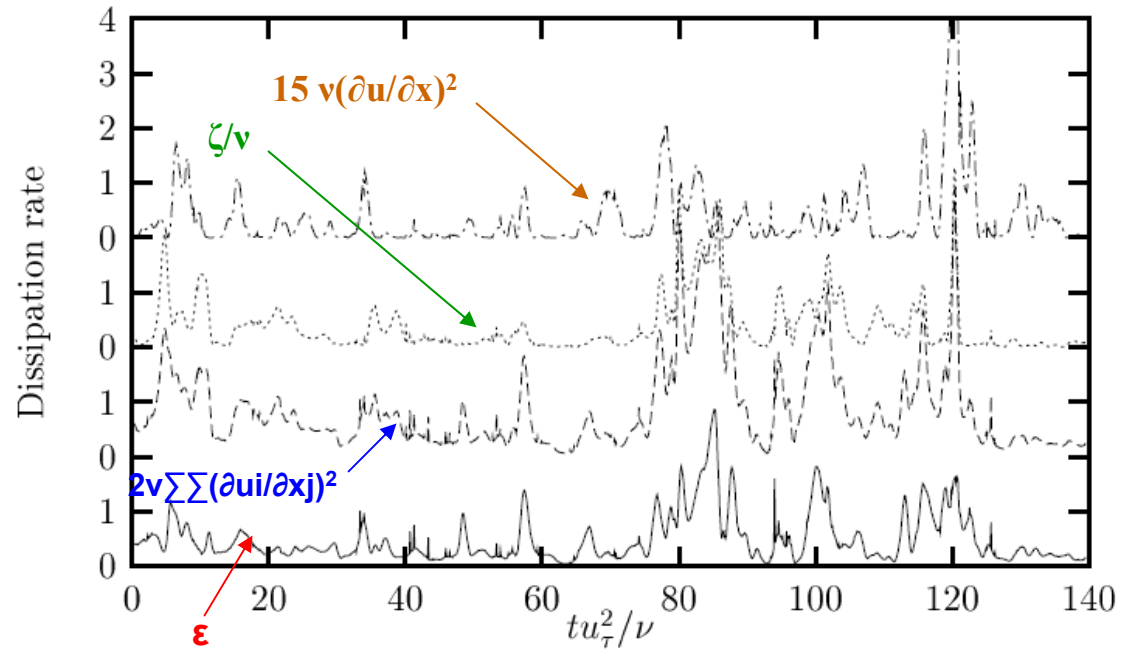
Dissipation Rate in Near-Surface of Atmospheric Boundary Layer



Dugway site southwest of Salt Lake City



$R_0 \approx 10^6$



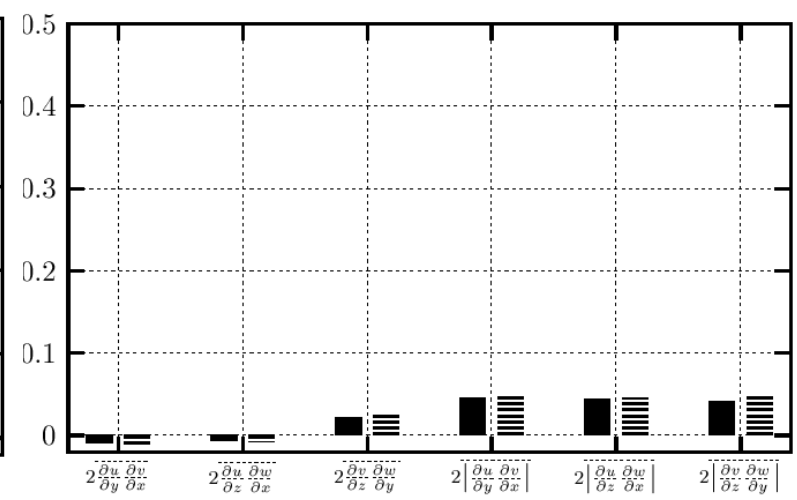
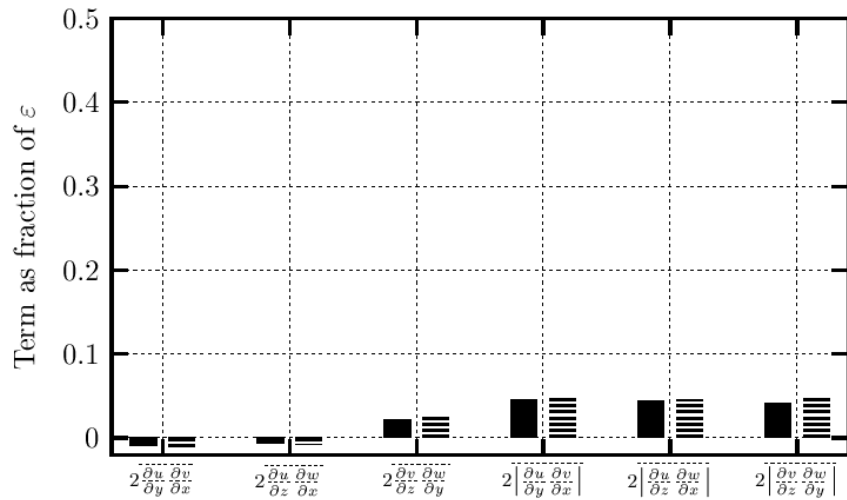
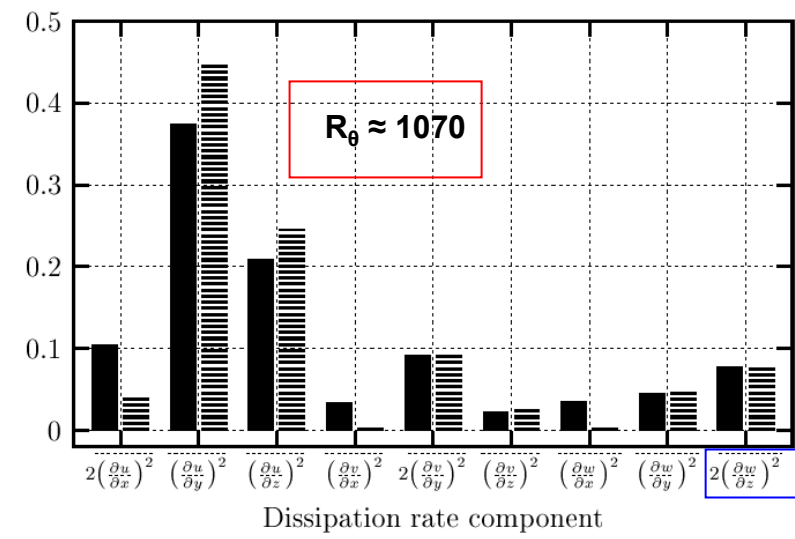
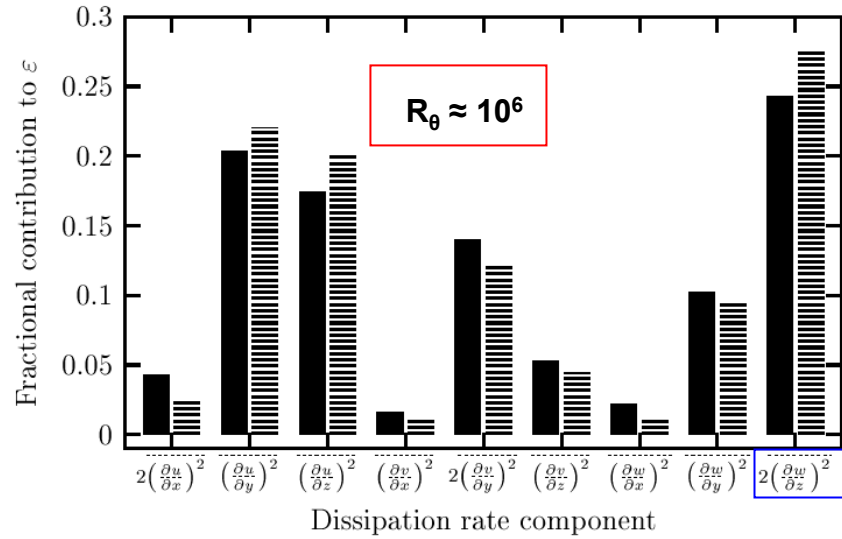
Folz (1997) Ph.D. Diss., Univ. of Maryland

An experimental study of the near-surface turbulence in the atmospheric boundary layer.



Dissipation Rate in Near-Surface of Atmospheric & Laboratory Boundary Layers

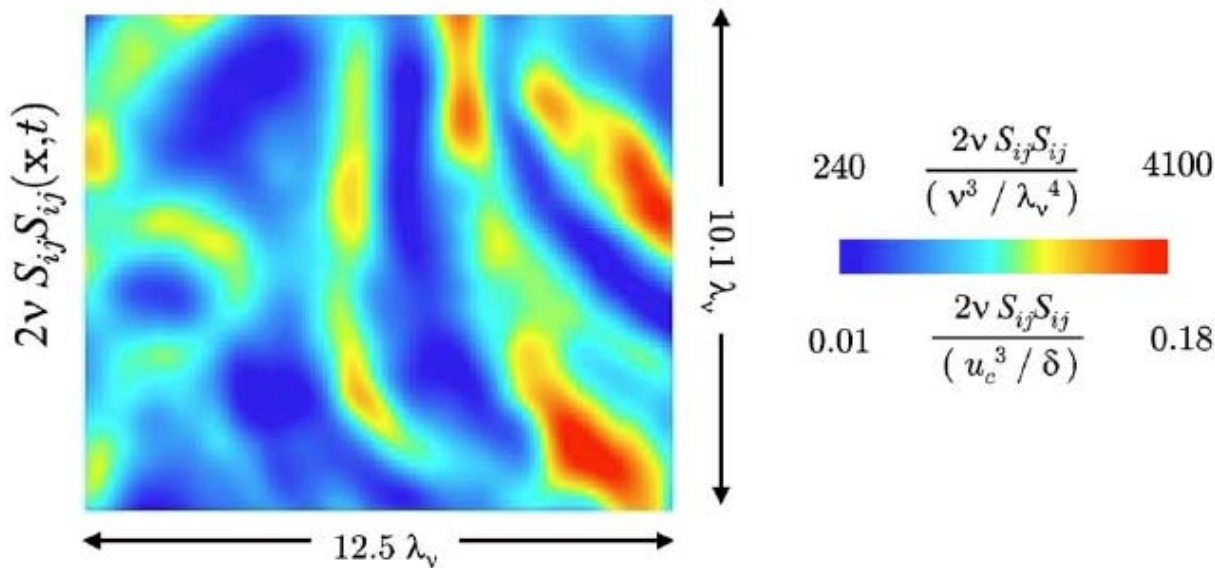
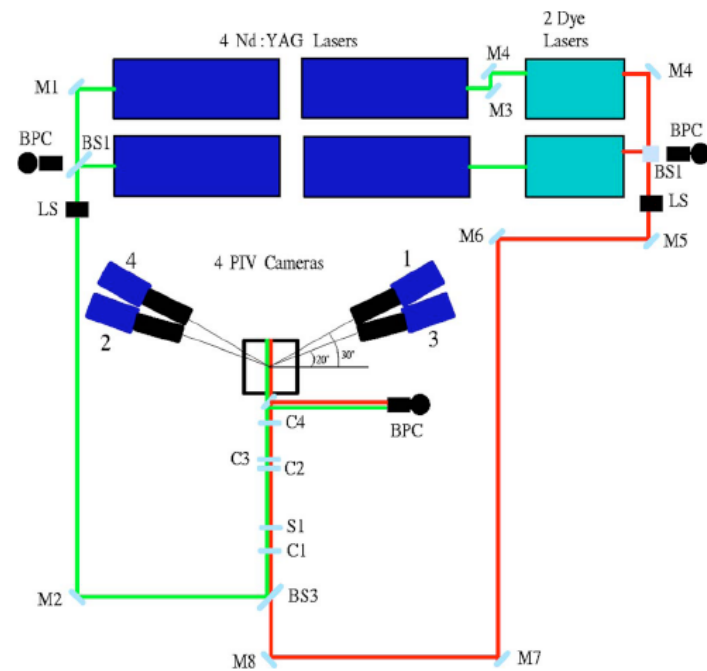
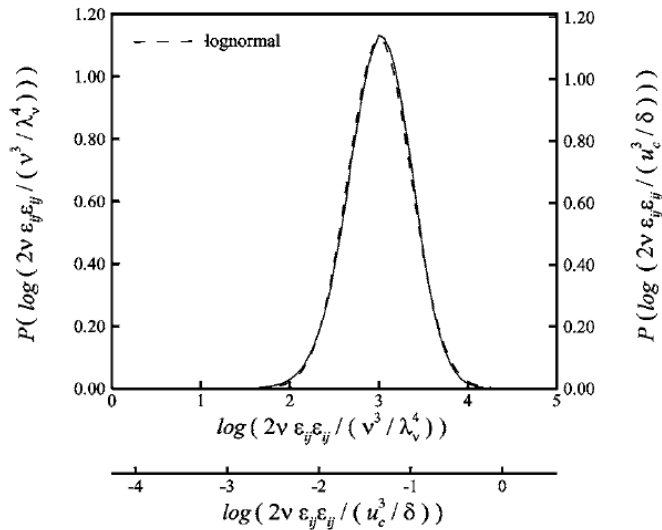
$y^+ = 45$





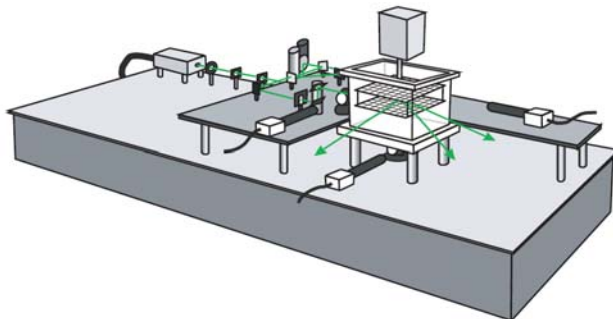
Dual Plane PIV Measurements of Dissipation Rate in a Turbulent Jet

J.A. Mullin & W.J.A. Dahm (2006)
Phvs. Fluids 18





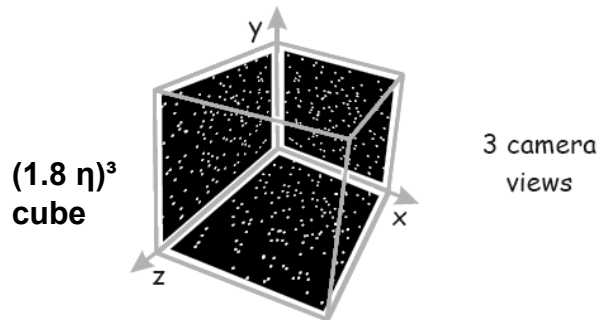
Particle Tracking Measurements of Dissipation Rate in a Turbulent Grid Flow



.4 .6 .8 1 2 4 6 8



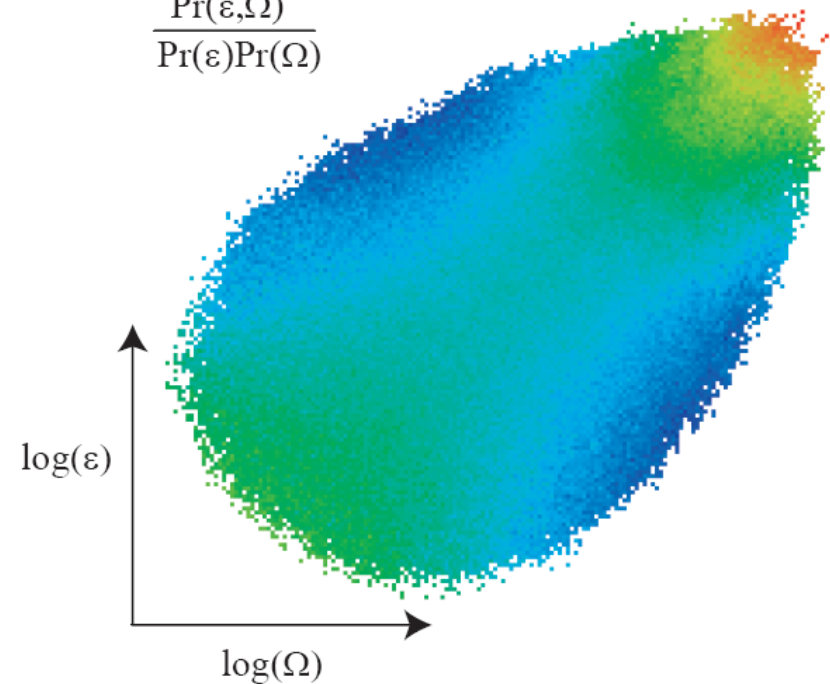
$$\frac{\text{Pr}(\varepsilon, \Omega)}{\text{Pr}(\varepsilon)\text{Pr}(\Omega)}$$



fit data to model

$$\vec{v} = \vec{v}_0 + \mathbf{M} \cdot \vec{x}$$

$$\mathbf{M} = \begin{bmatrix} \partial_x v_x & \partial_y v_x & \partial_z v_x \\ \partial_x v_y & \partial_y v_y & \partial_z v_y \\ \partial_x v_z & \partial_y v_z & \partial_z v_z \end{bmatrix}$$



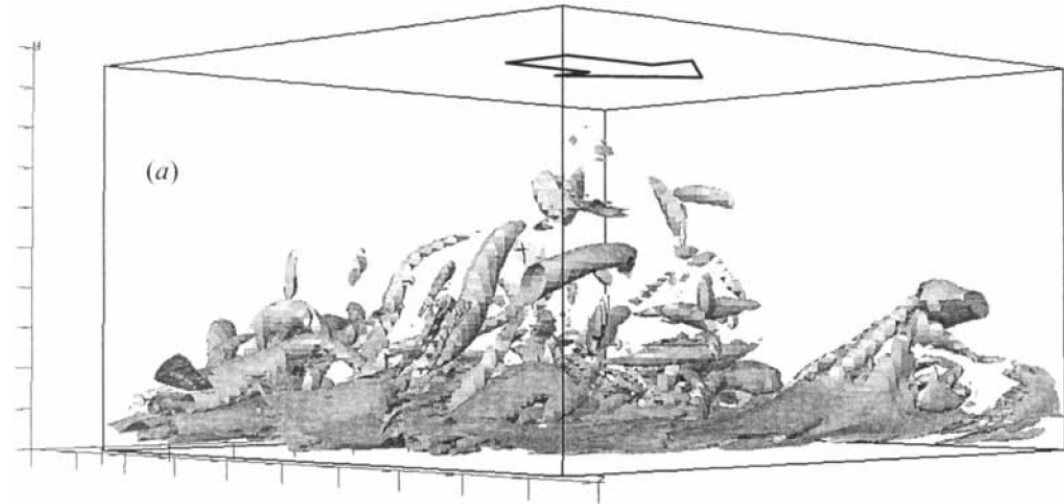
B. W. Zeff, D. D. Lanterman, R. McAllister, R. Roy, E. J. Kostelic & D. P. Latrop (2003)

Nature 421.

Visualization of Enstrophy and Dissipation Rate in a Channel Flow DNS

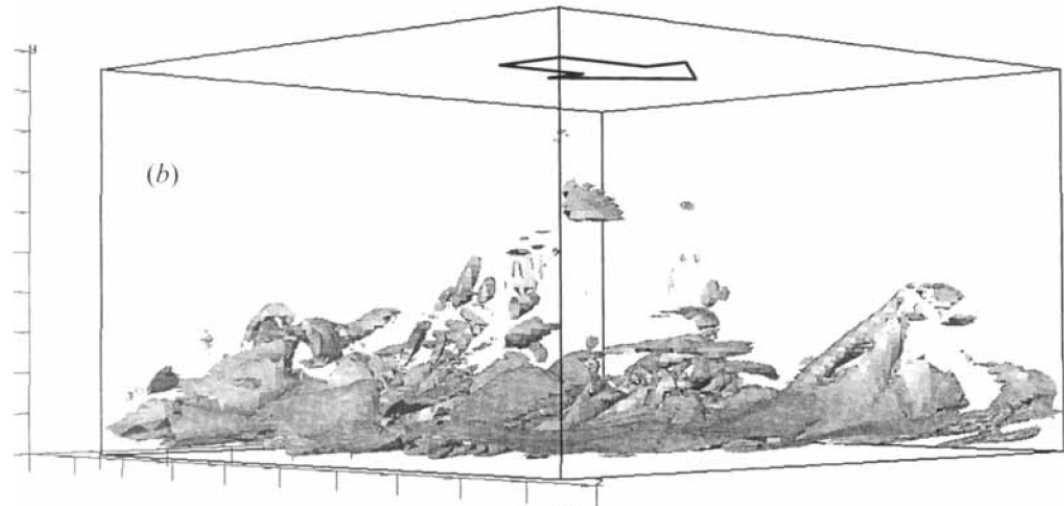


Iso-surfaces of enstrophy



Iso-surfaces of dissipation rate

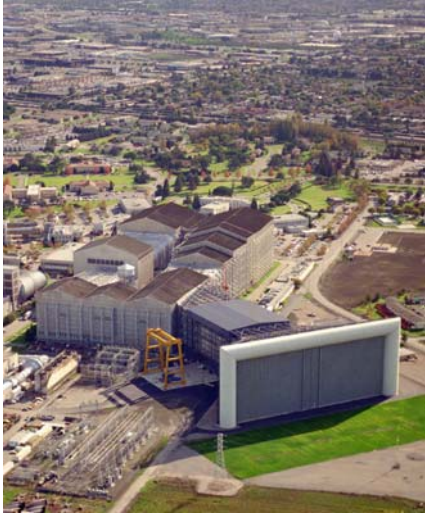
$\varepsilon = \nu \xi$ for homogeneous
turbulence



Blackburn, N.N. Mansour
& B.J. Cantwell (1996)
JFM 310

Box of size $\Delta x^+ = 670$, $\Delta y^+ = 375$, $\Delta z^+ = 640$

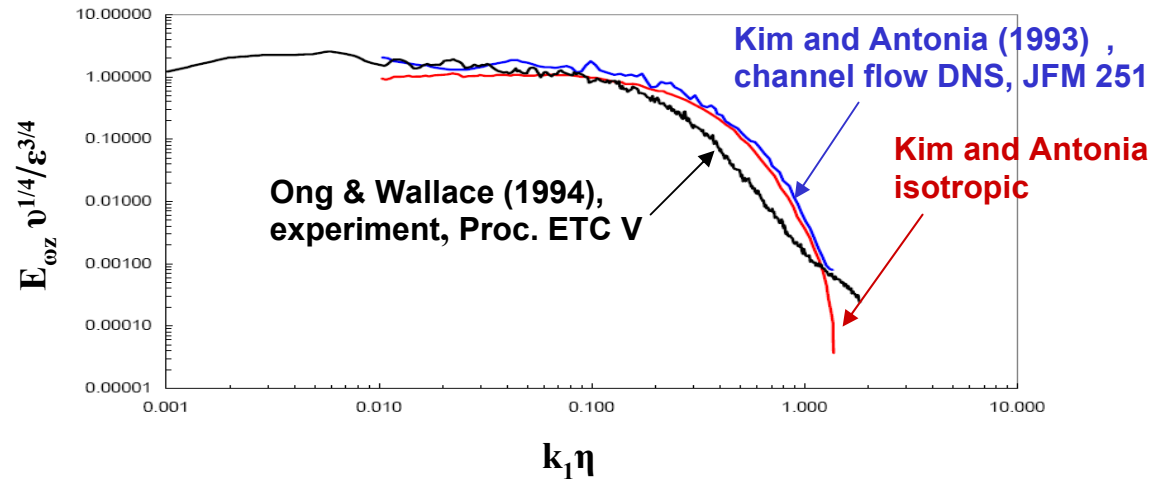
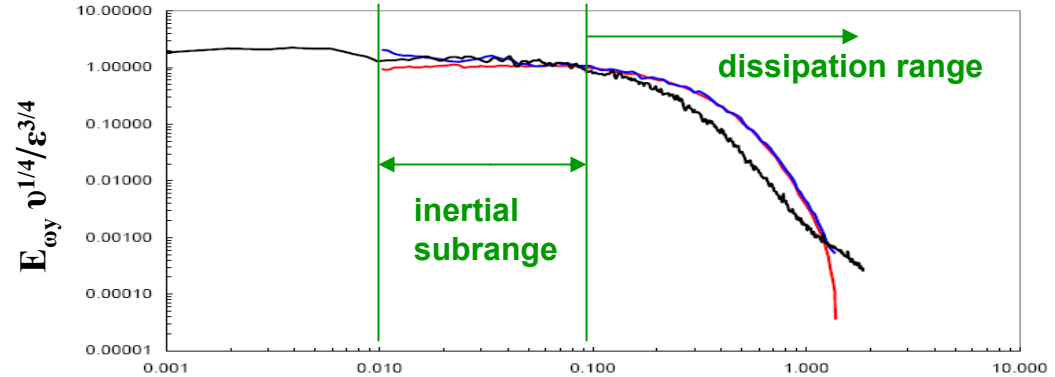
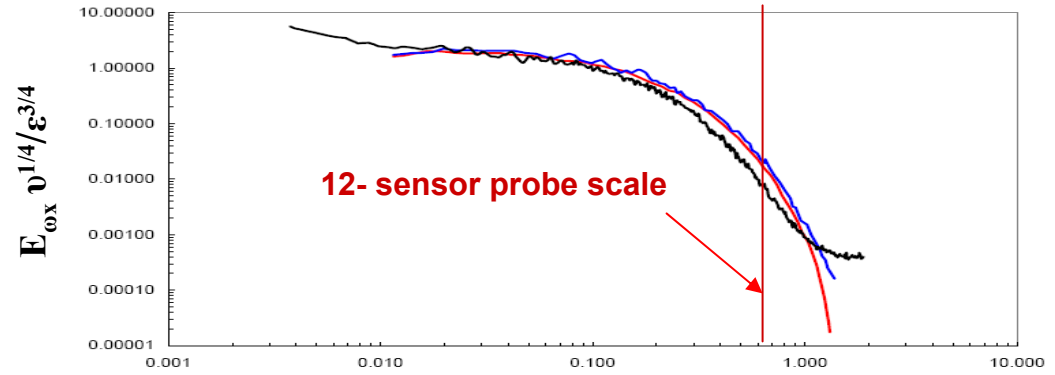
Local Isotropy of the Vorticity Field in a High Reynolds Number Turbulent Boundary Layer



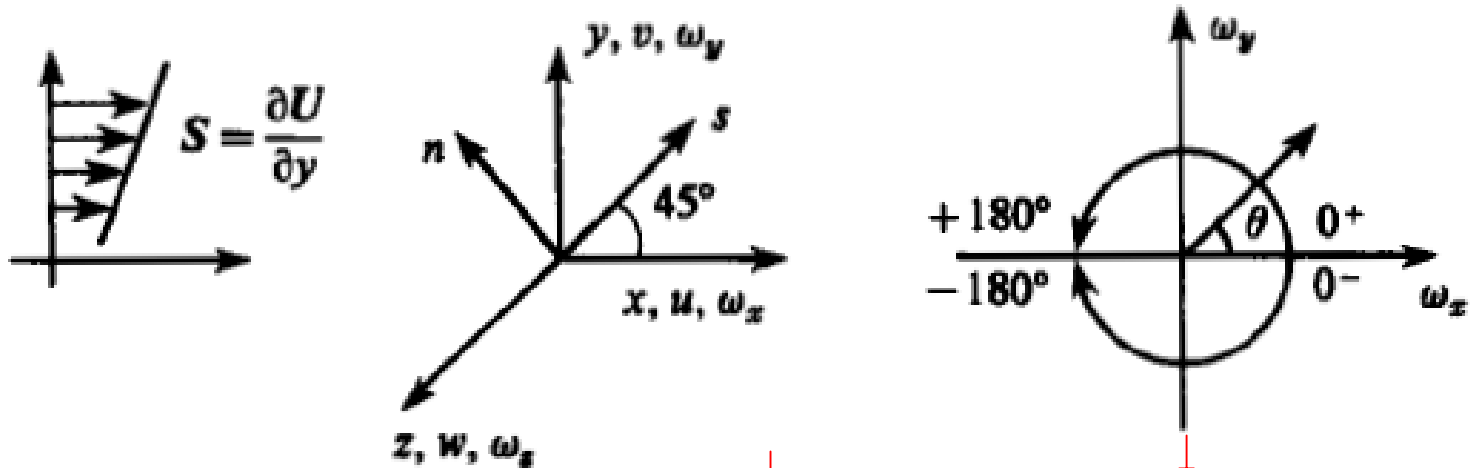
NASA Ames 80' x 120' Wind Tunnel



probe location

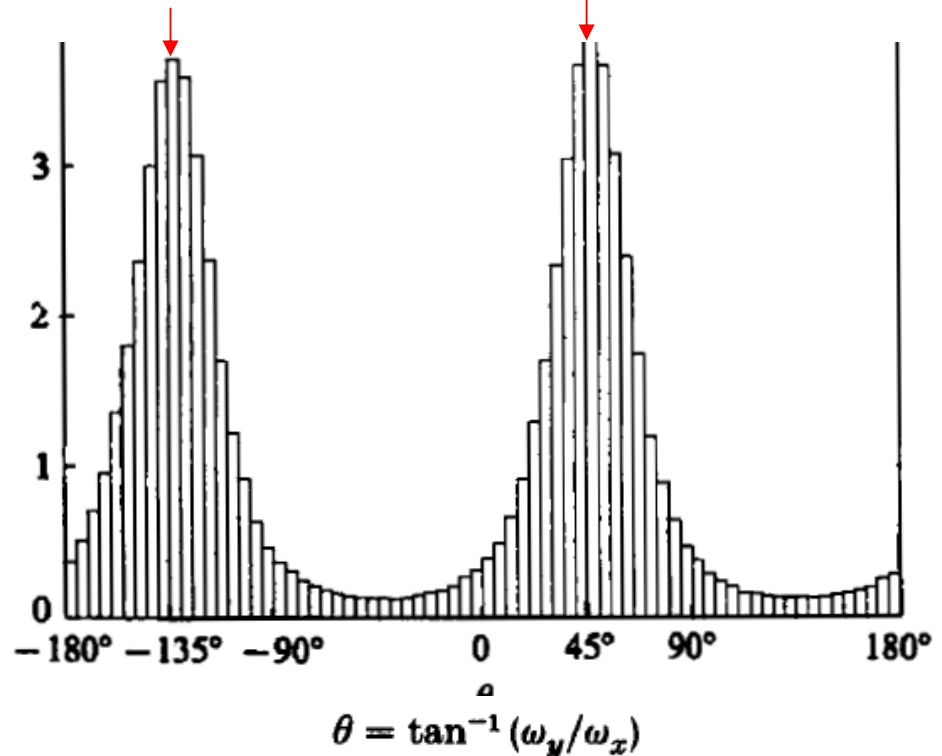


Orientation of the Vorticity Vector in Homogeneous Turbulent Shear Flow



The distribution of the **inclination angle** of the projection of the vorticity vectors in the x-y streamwise plane. Data weighted with the magnitude of the projected vorticity $(\Omega_x^2 + \Omega_y^2)^{1/2}$.

Distribution attains rather sharp maxima at **45°** and **-135°** (the direction of principal elongation by the mean strain). $R_\lambda = 14.2$



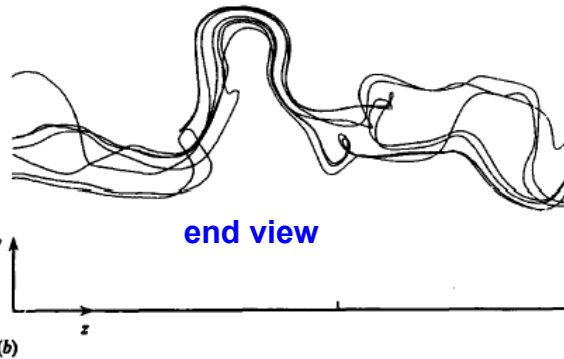
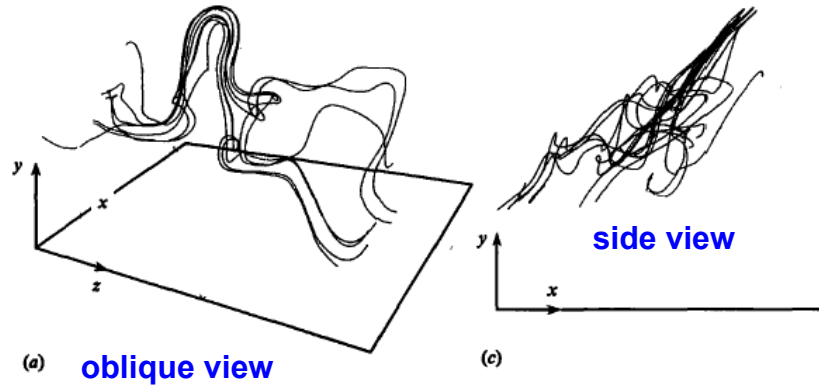
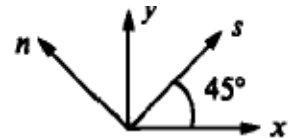
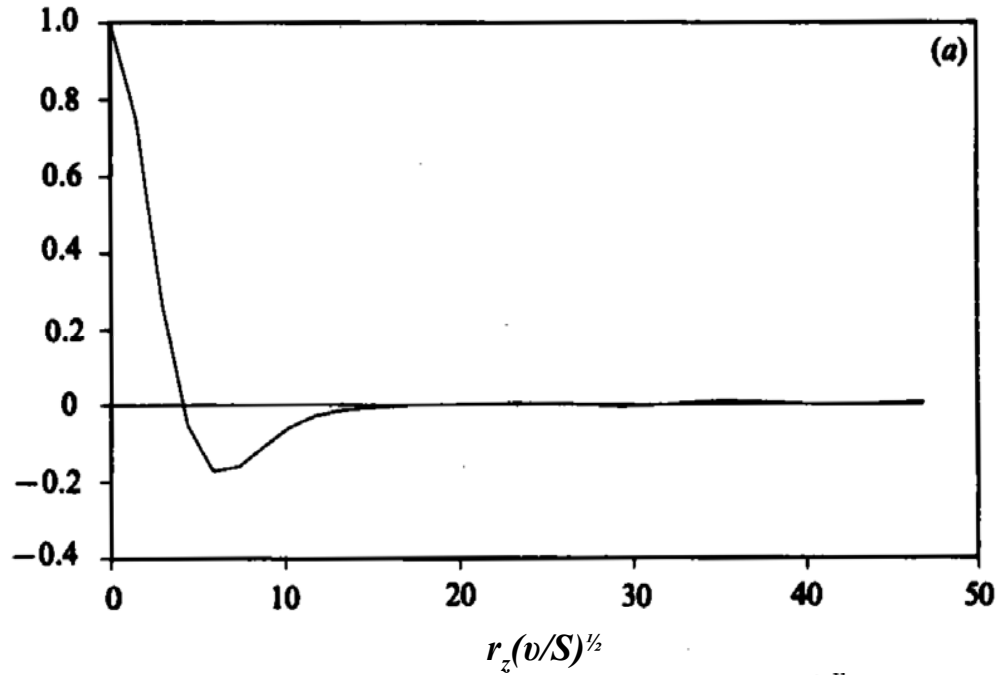


Vortex Lines and Vorticity Component Correlation

Two-point correlation of ω_s vorticity component with spanwise separation

$$R_{\omega_s \omega_s}$$

Hairpin Shaped vortex Lines

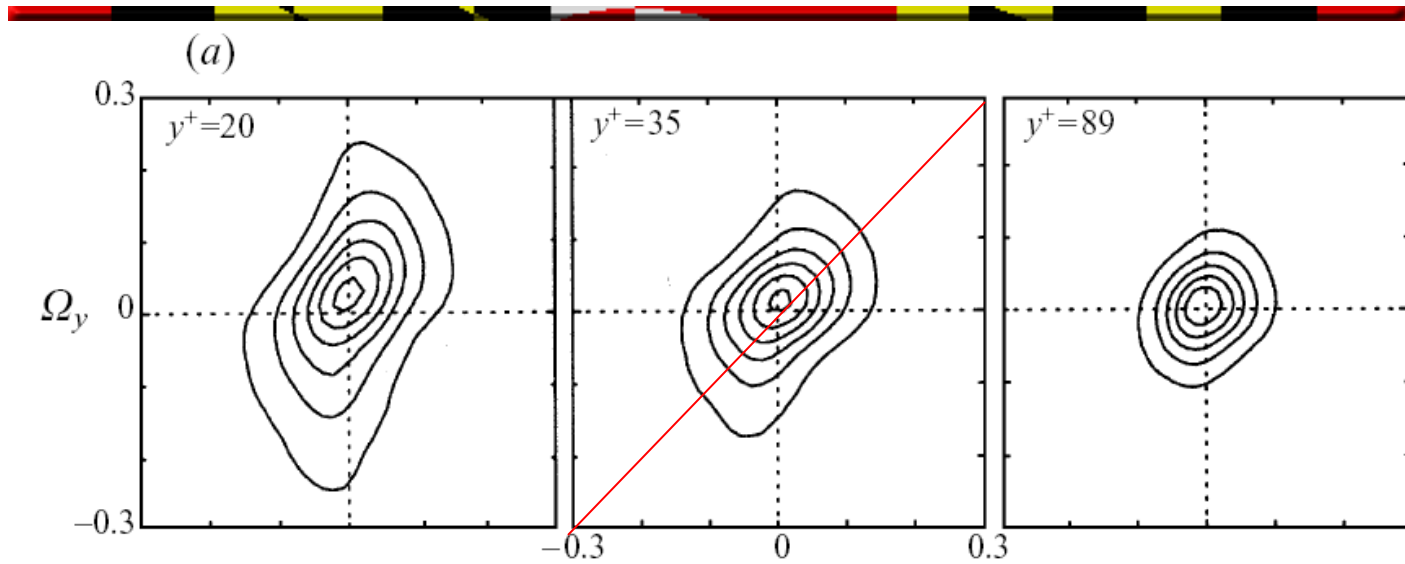


M. M. Rogers & P. Moin
(1987)
JFM 176

Orientation of the Vorticity Vector in a Turbulent Boundary Layer

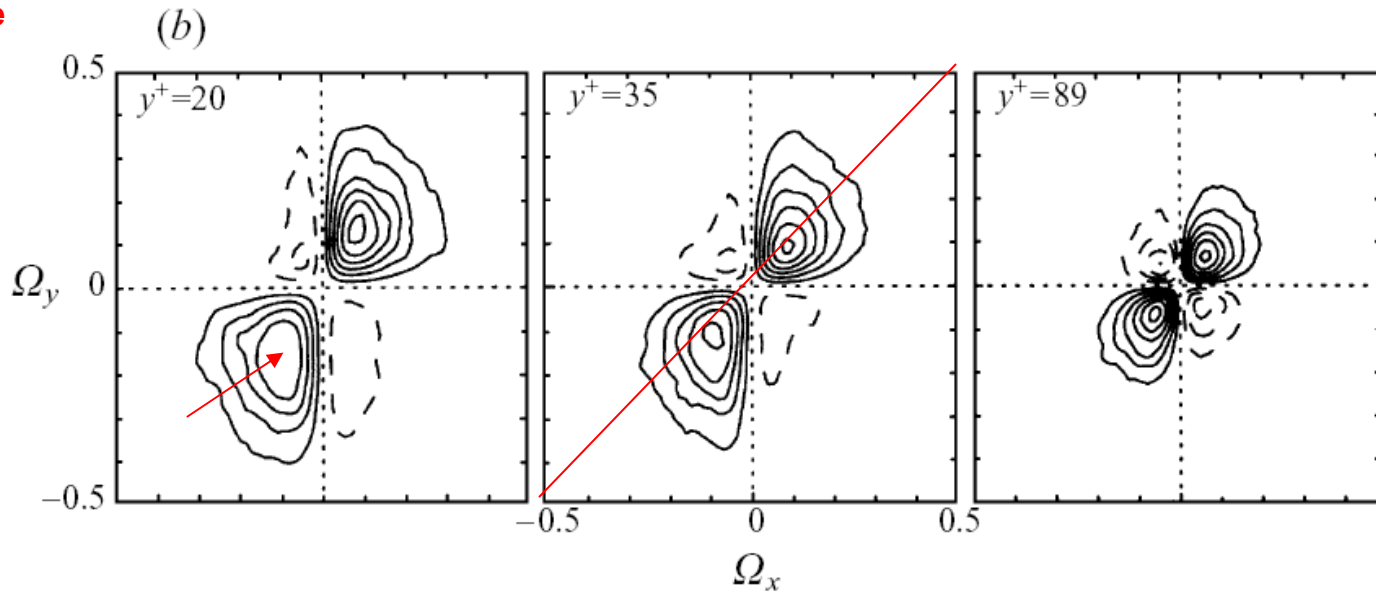


JPDFs
 $P(\Omega_x, \Omega_y)$



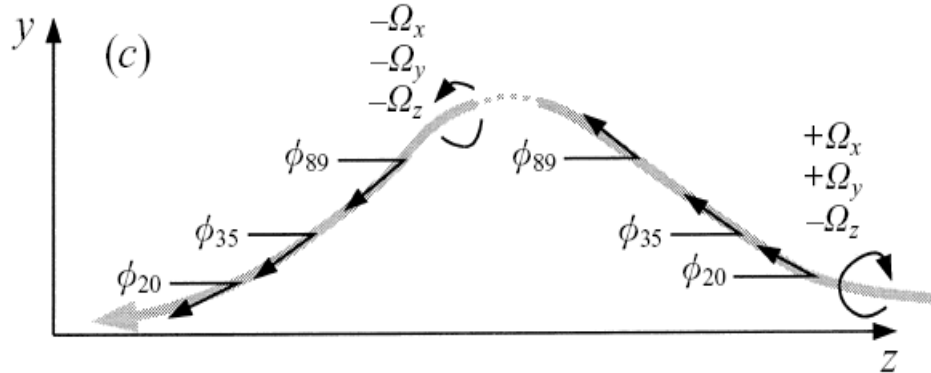
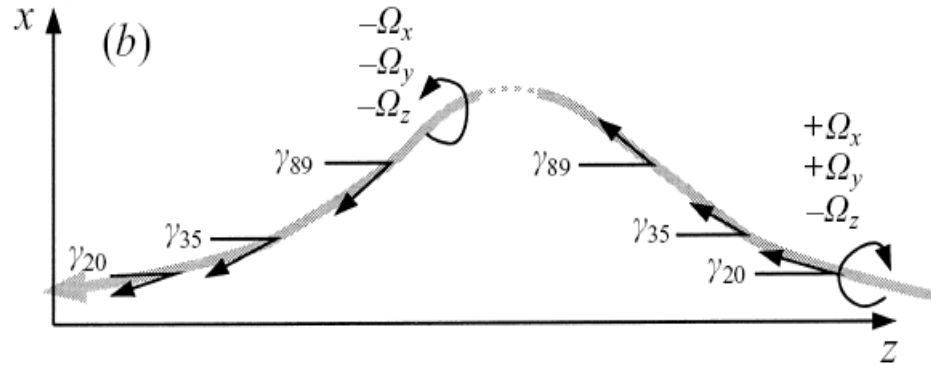
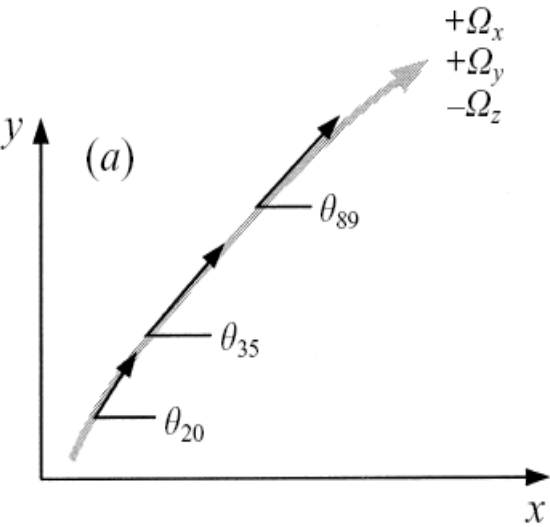
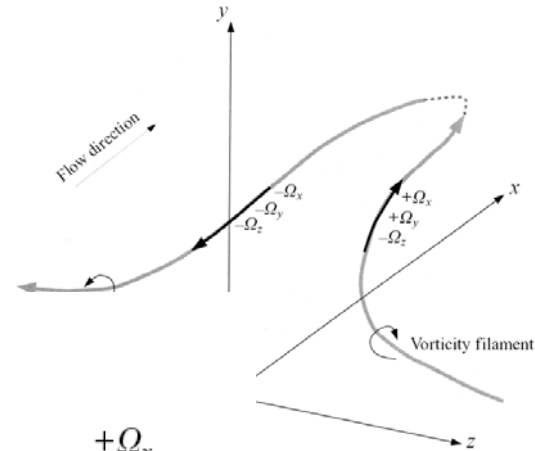
Streamwise x-y Plane

Covariance
Integrands
 $\Omega_x \Omega_y P(\Omega_x, \Omega_y)$





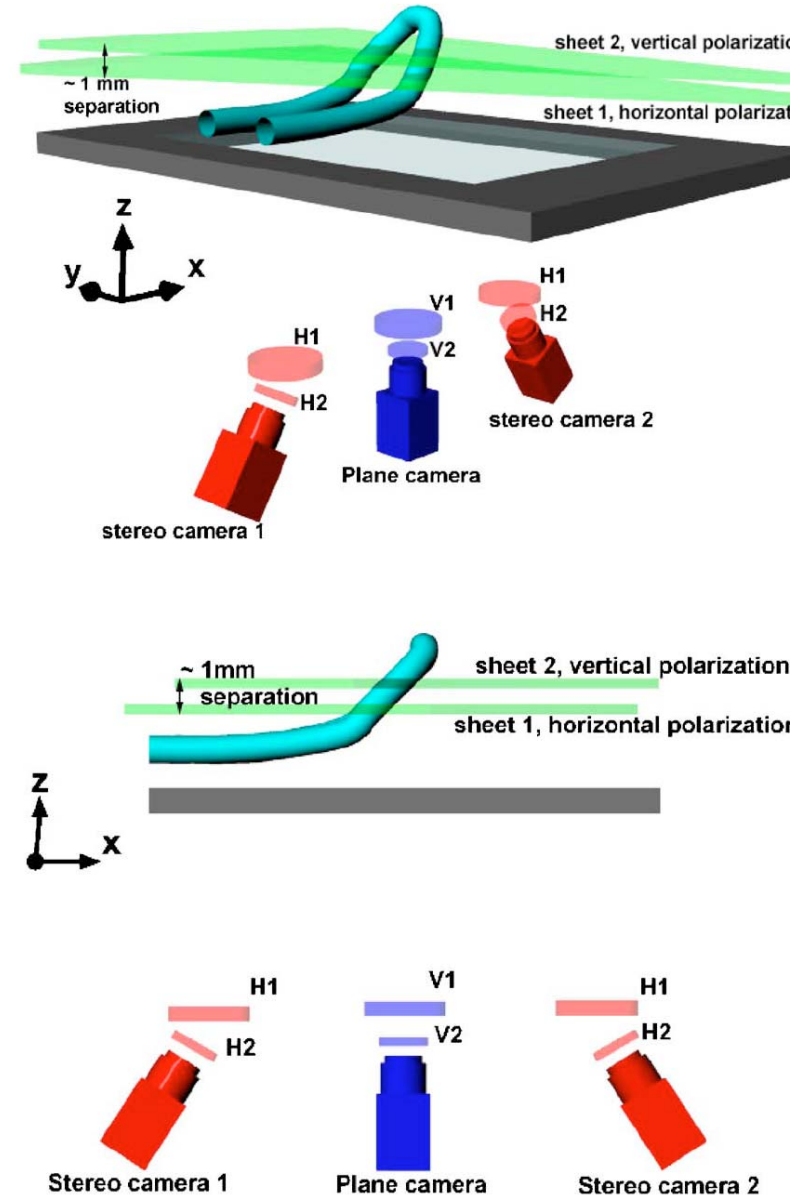
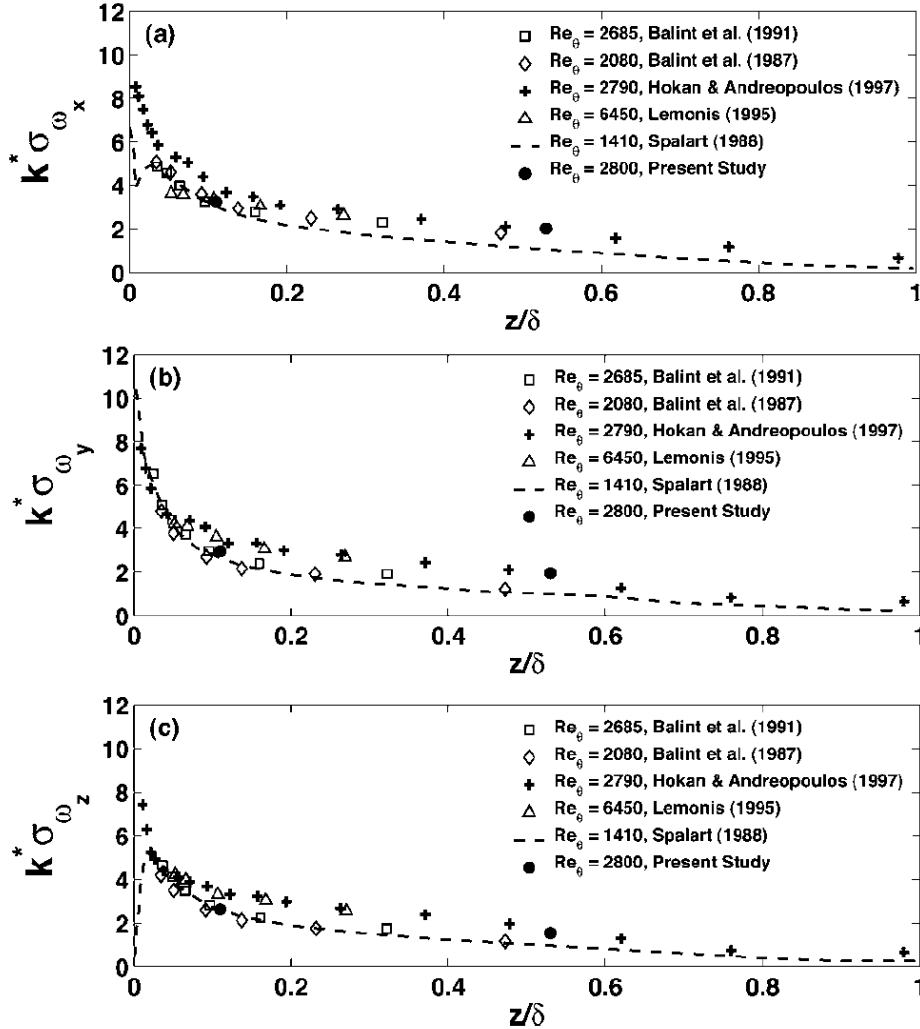
Vorticity Filaments and Vorticity Covariances



Projections of vorticity filament segments making the largest contributions to the vorticity covariances

$$\langle \Omega_x \Omega_y \rangle = \int \Omega_x \Omega_y P(\Omega_x, \Omega_y) d\Omega_x d\Omega_y$$

PIV Study of Vortices in a Turbulent Boundary Layer

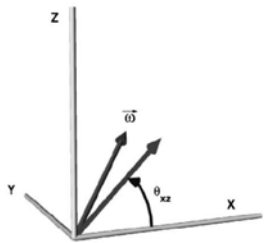


B. Ganapathisubramani, E. Longmire & I. Marusic
Phys. Fluids 18 (2006)

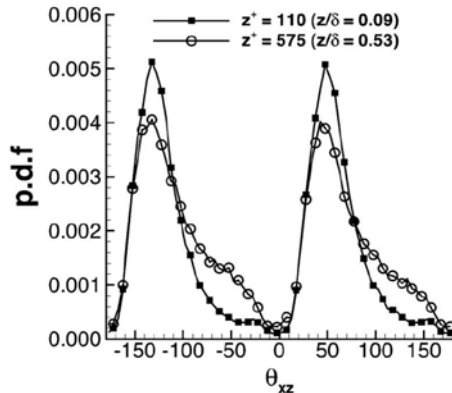
PIV Study of Vortices in a Turbulent Boundary Layer



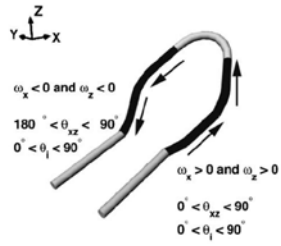
B. Ganapathisubramani, E. Longmire
& I. Marusic
Phys. Fluids 18 (2006)



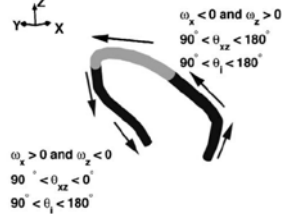
(a)



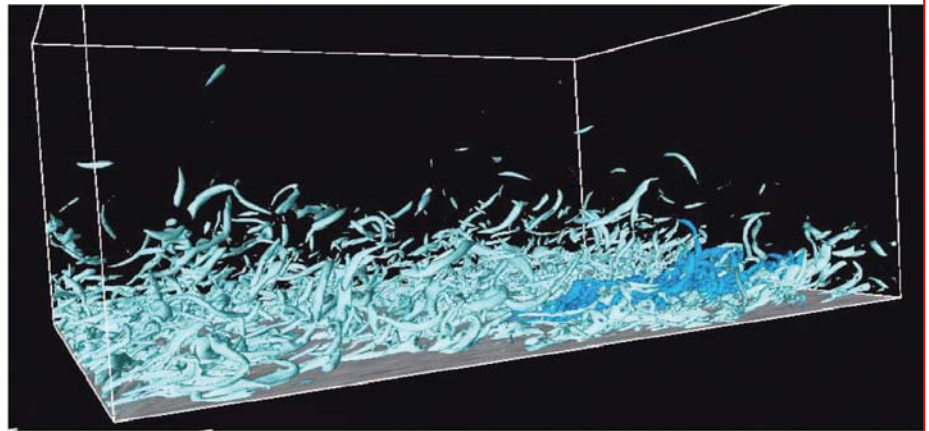
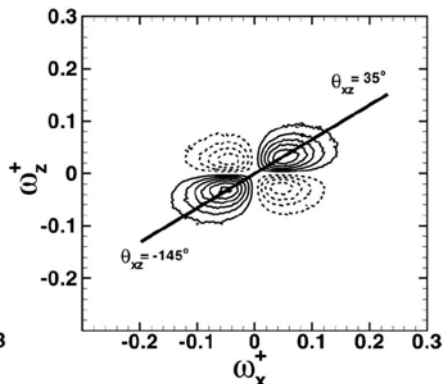
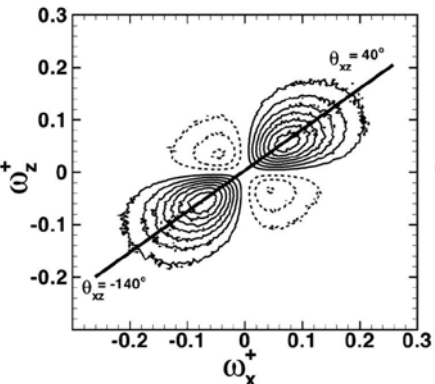
(b)



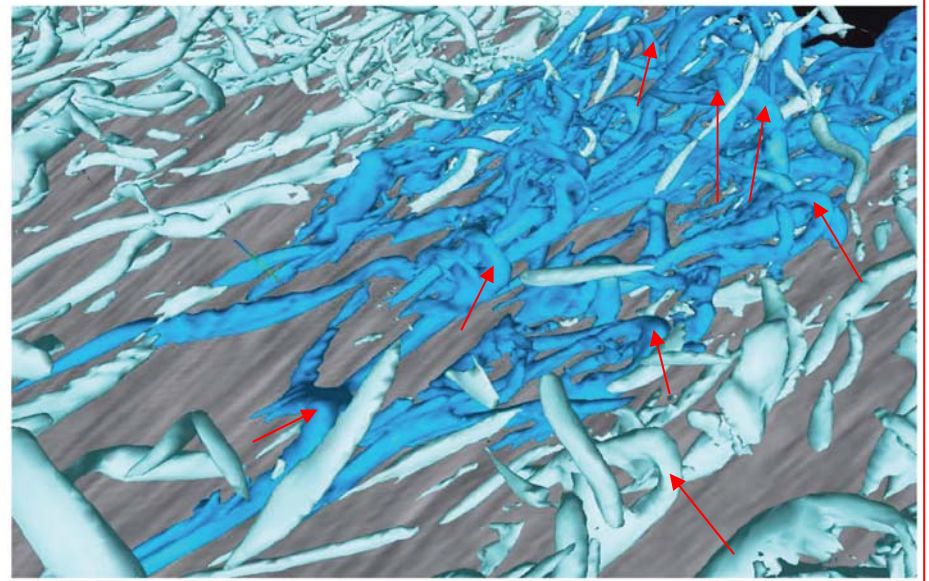
(c)



(d)



(a)



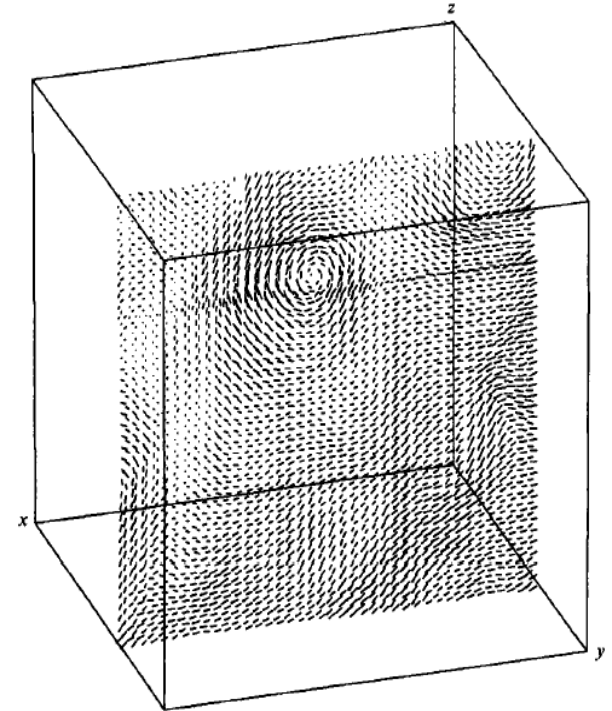
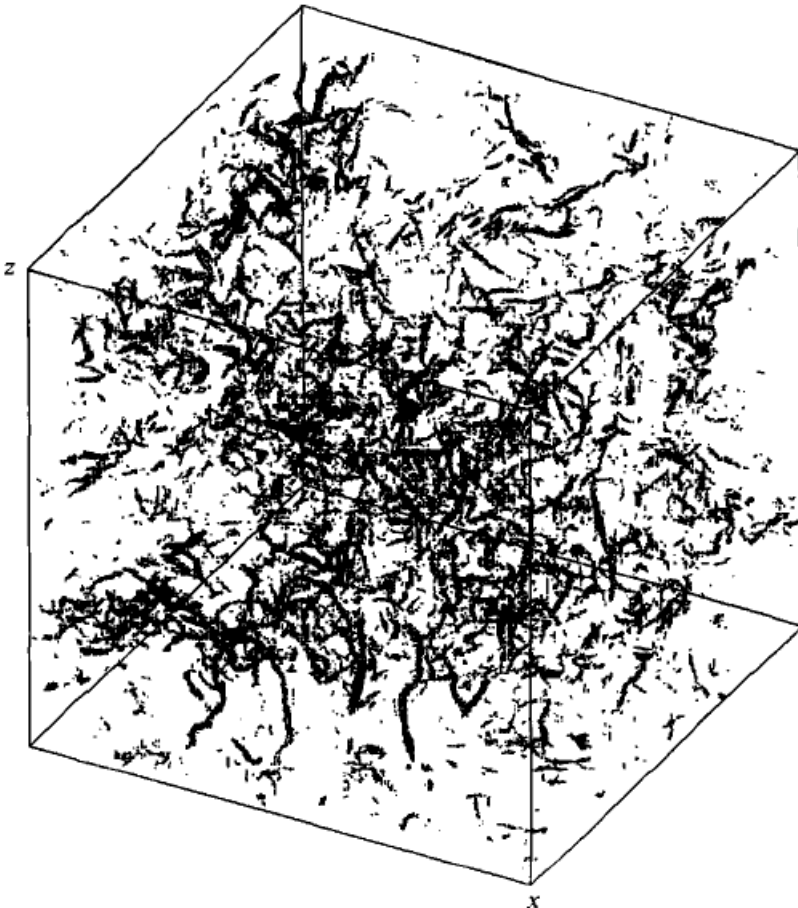
△ vortex identifier applied to channel flow DNS of
J. Del Alamo, J. Jimenez, P. Zandonade & R. Moser
J. Fluid Mech. 500 (2004)



Vorticity Tubular “Worms” in Isotropic Turbulence

Vorticity field in DNS of isotropic turbulence at $R_\lambda = 150$.
Vector length proportional to the vorticity magnitude at each grid point.

“Vorticity is organized in thin elongated tubes...Their thickness is of the order of a few dissipation scales...”



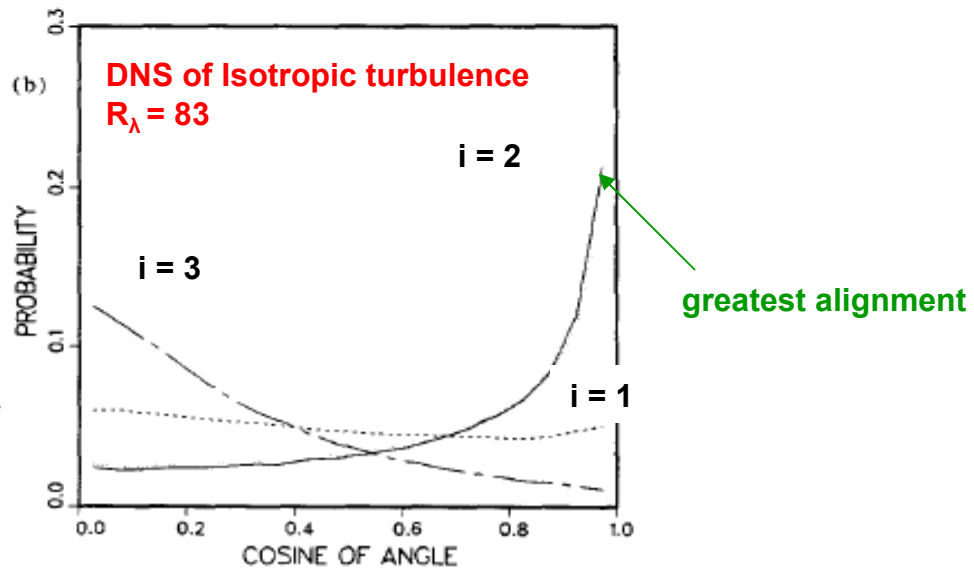
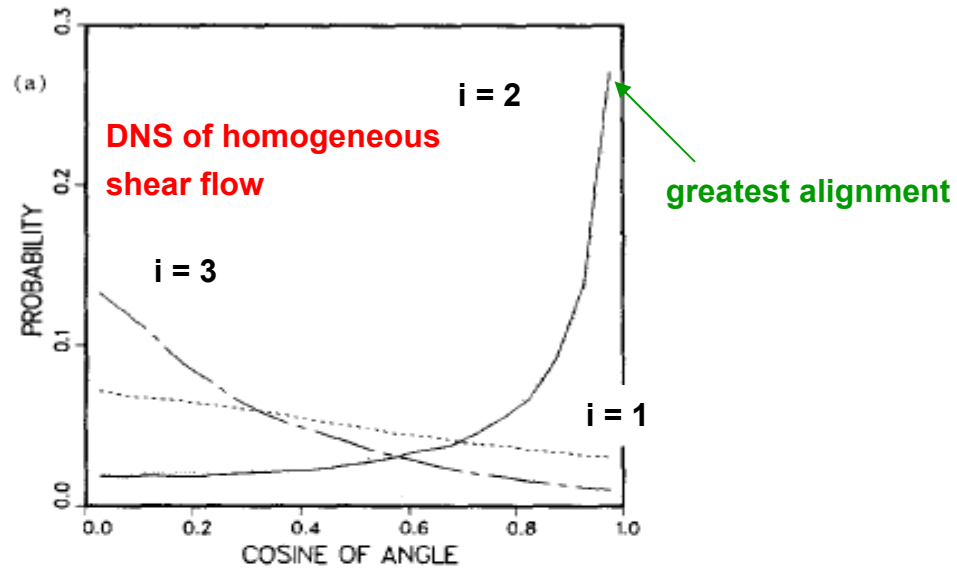
Projection of the velocity field perpendicular to a single vorticity tube

Vincent & M. Meneguzzi (1991)
JFM 225

Alignment of Vorticity Vector with Eigenvectors of Rate-of-Strain Tensor



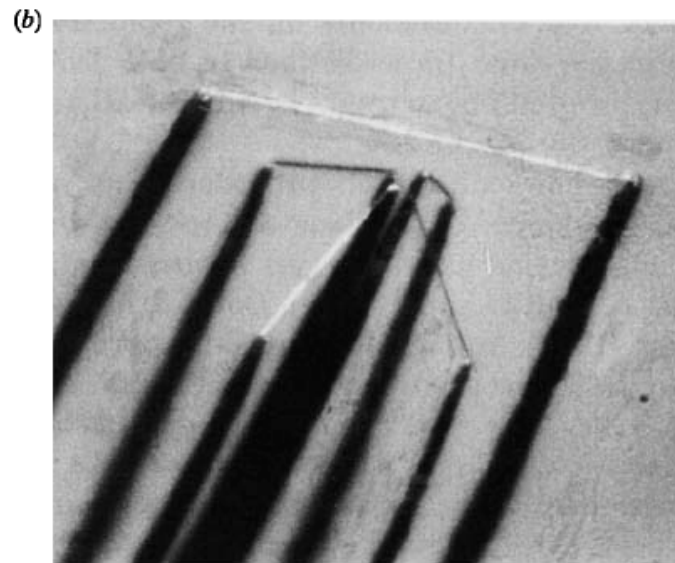
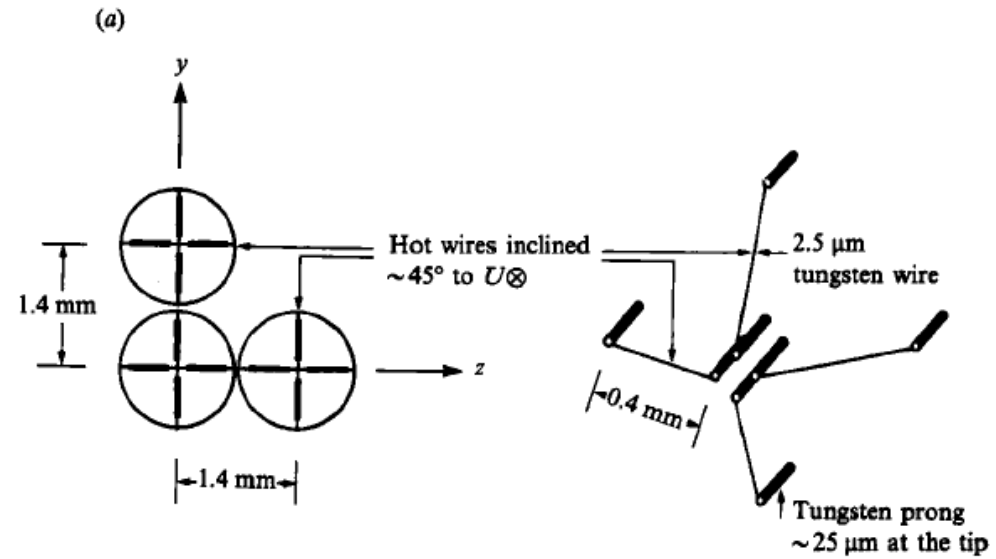
PDFs of cosine of angle between vorticity vector and eigenvectors of the rate-of-strain tensor, α_i



Wm. T. Ashurst, A. R. Kerstein, R. M. Kerr
and C. H. Gibson (1987)
Phys. Fluids 30



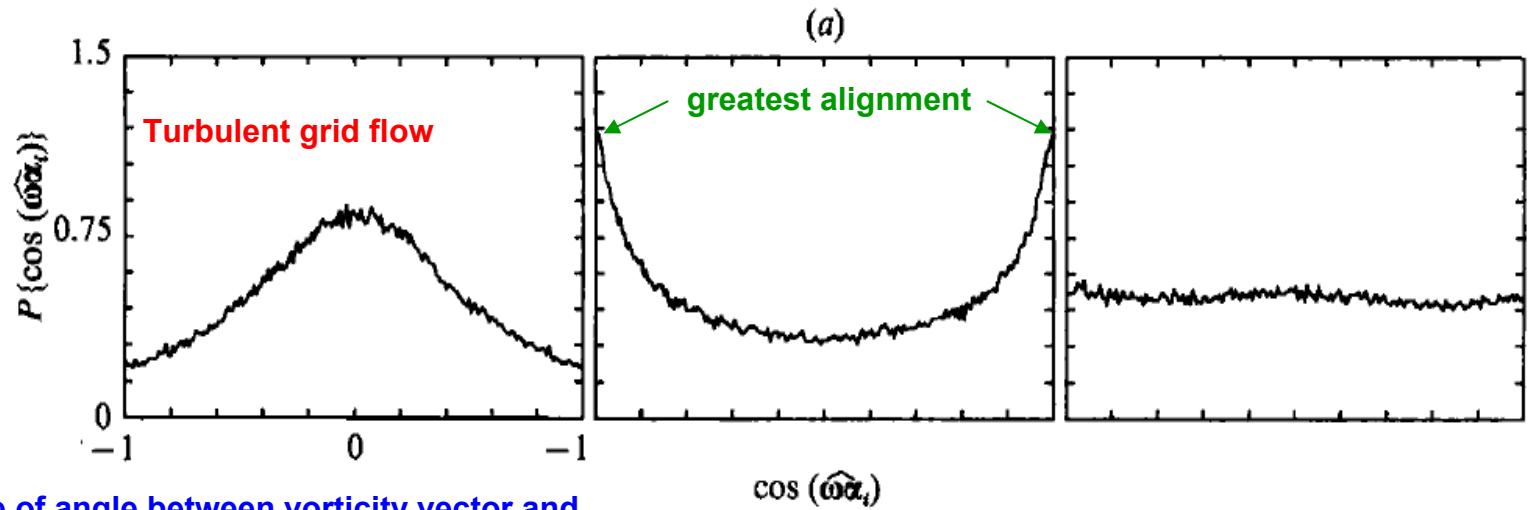
12-Sensor Hot-Wire Probe



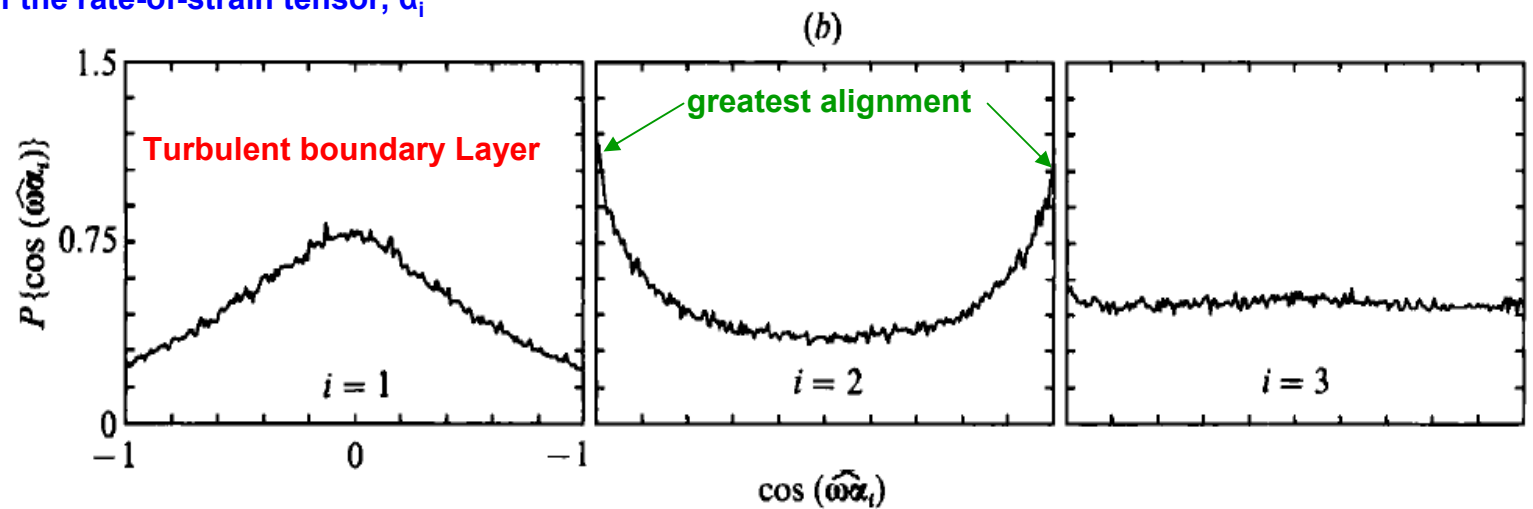
Tsinober, E. Kit & T. Dracos (1992)
JFM 242



Alignment of Vorticity Vector with Eigenvectors of Rate-of-Strain Tensor



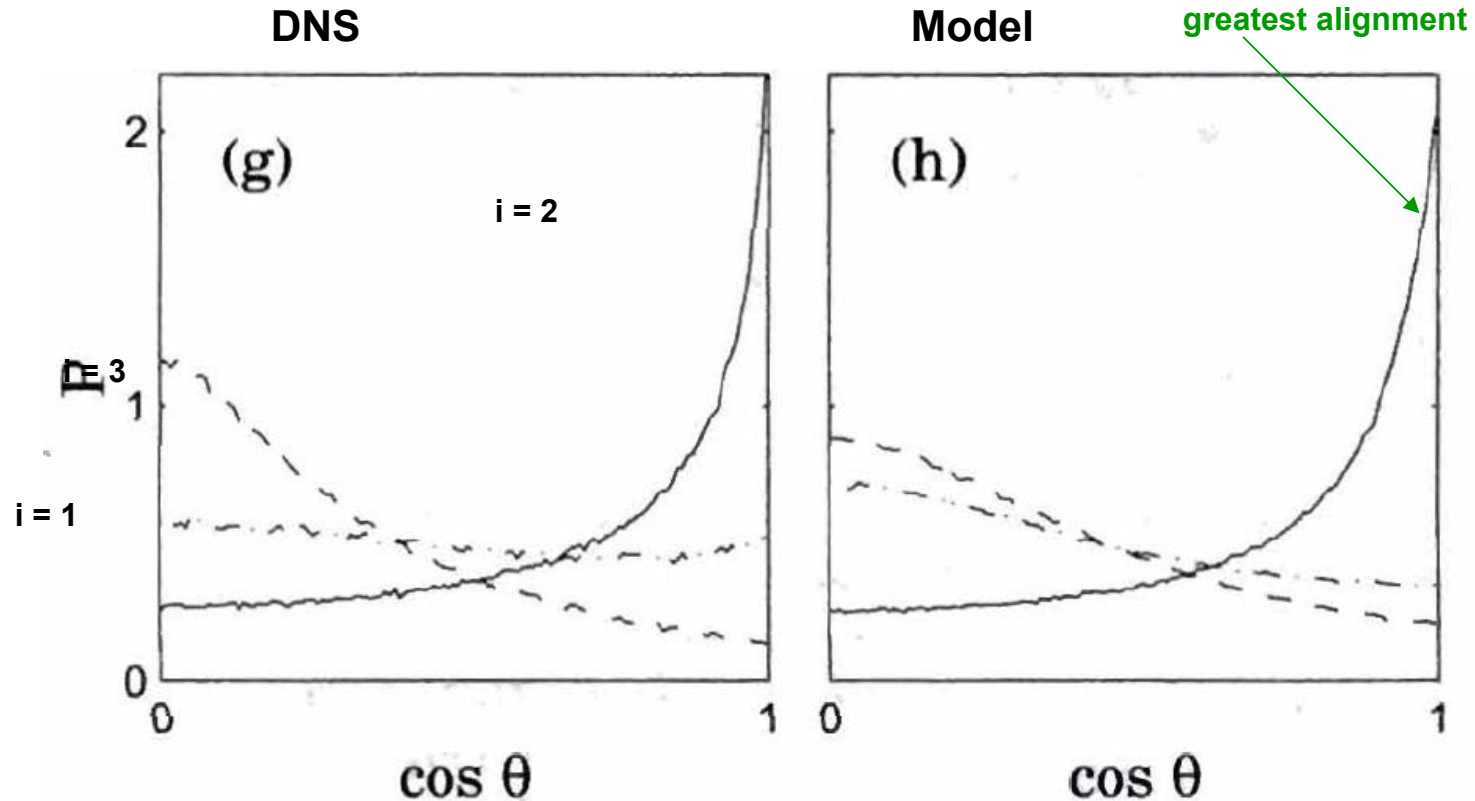
PDFs of cosine of angle between vorticity vector and eigenvectors of the rate-of-strain tensor, α_i





Alignment of Vorticity Vector with Eigenvectors of Rate-of-Strain Tensor

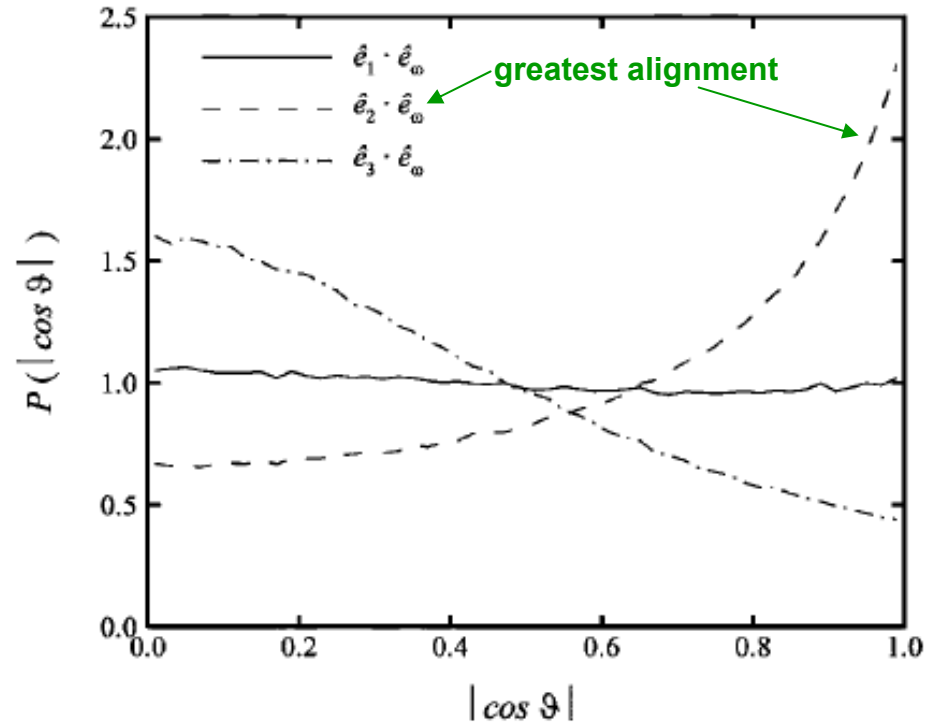
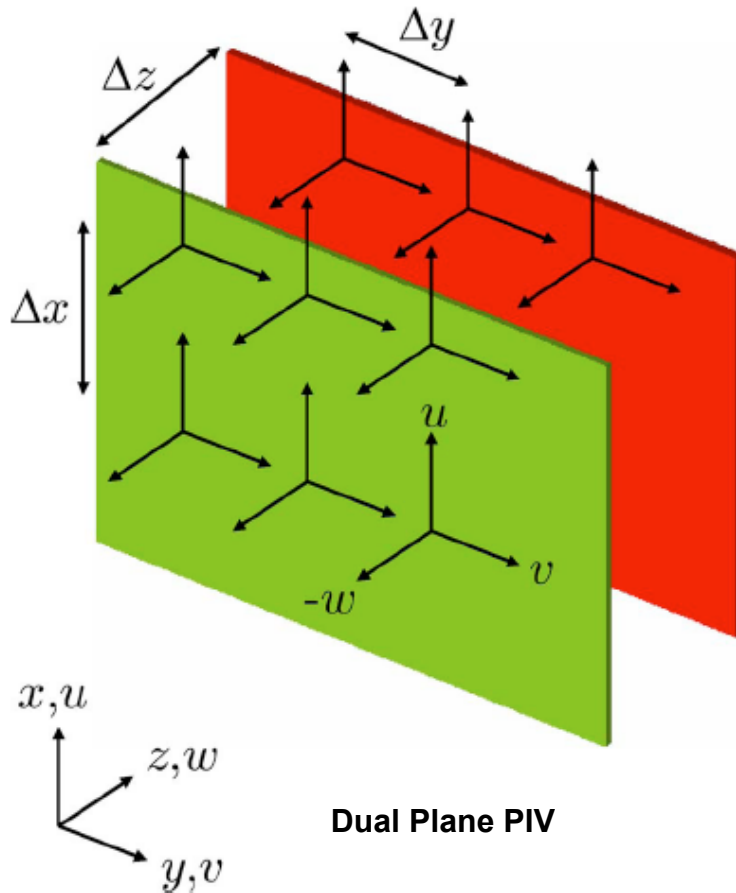
Model is of the time evolution of the A_{ij} along Lagrangian Trajectories with closures of the pressure Hessian and The viscous Laplacian



L. Chevillard, C. Meneveau, L. Biferale & F. Toschi (2008)
Phys. Fl. (to be published)



Alignment of Vorticity Vector with Eigenvectors of Rate-of-Strain Tensor



J.A. Mullin & W.J.A. Dahm (2006)
Phys. Fluids 18

JPDF of the Q and R invariants of the Velocity Gradient Tensor A_{ij}



Data from throughout $R_0 = 670$ boundary layer DNS of Spalart

$A_{ij} = \partial U_i / \partial x_j = S_{ij} + R_{ij}$ (velocity gradient tensor)

$S_{ij} = \frac{1}{2}(\partial U_i / \partial x_j + \partial U_j / \partial x_i)$ (strain rate)

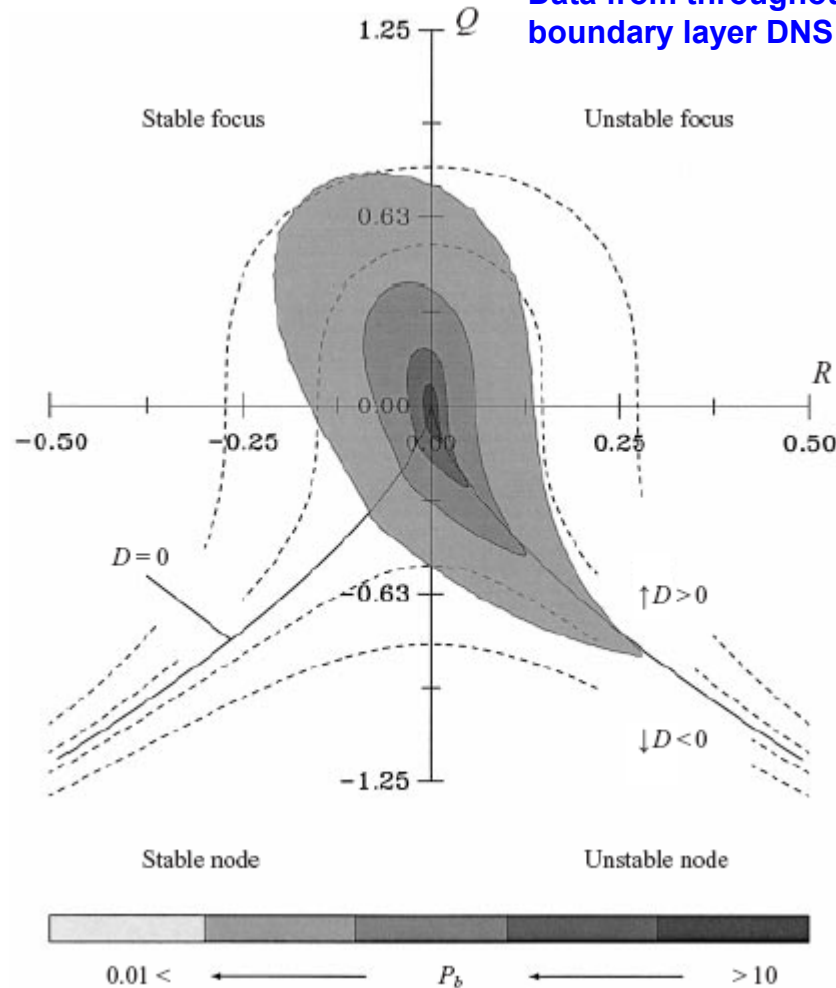
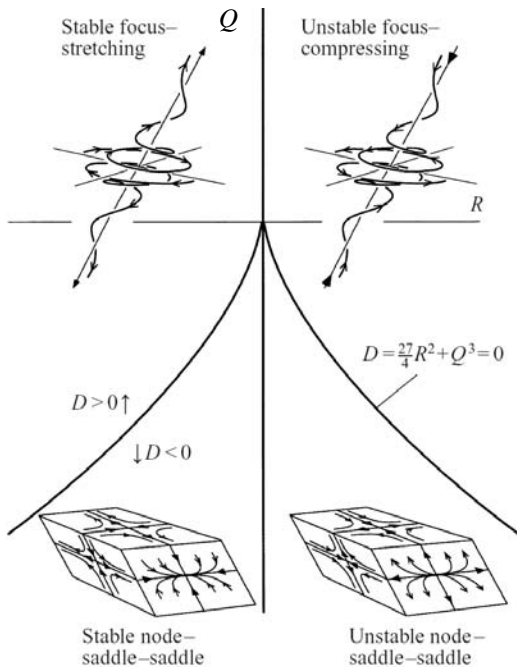
$R_{ij} = \frac{1}{2}(\partial U_i / \partial x_j - \partial U_j / \partial x_i)$ (rotation rate)

$\lambda^3 + P\lambda^2 + Q\lambda + R = 0$ (characteristic eqn of A_{ij})

$P = -S_{ii} = 0$ (for incompr. Flow)

$Q = \frac{1}{2}(-S_{ij}S_{ij} + R_{ij}R_{ij})$

$R = -\frac{1}{3}(S_{ij}S_{jk}S_{ki} + 3R_{ij}R_{jk}S_{ki})$



J.M. Chaćin & B. J. Cantwell (2000)
JFM 404

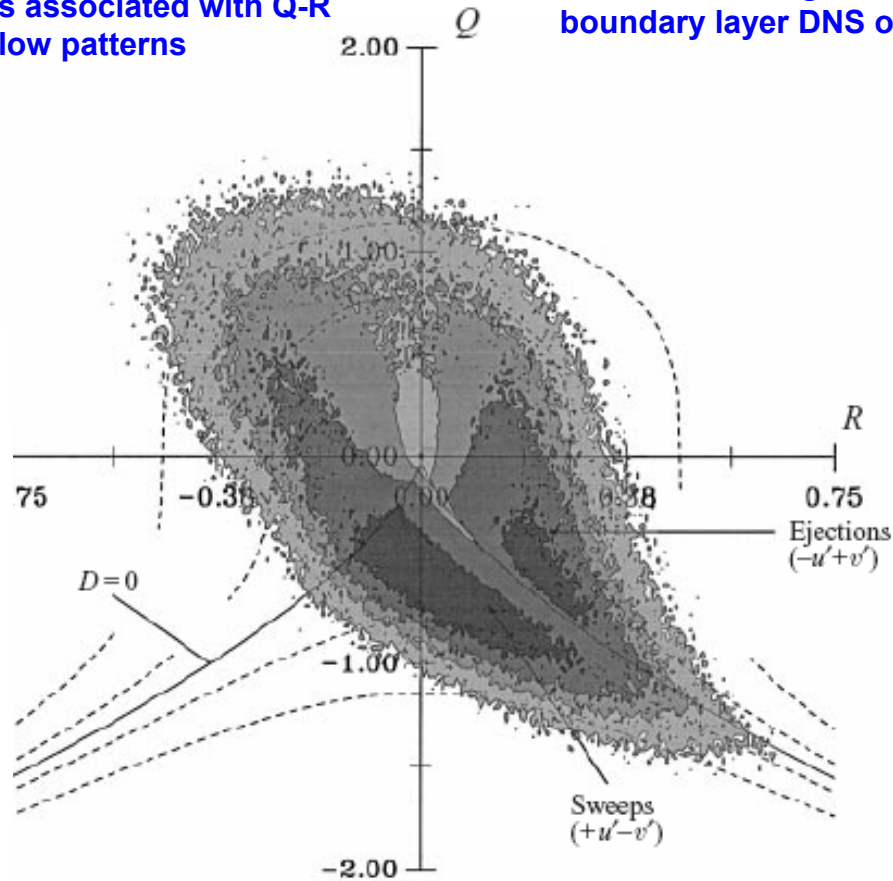
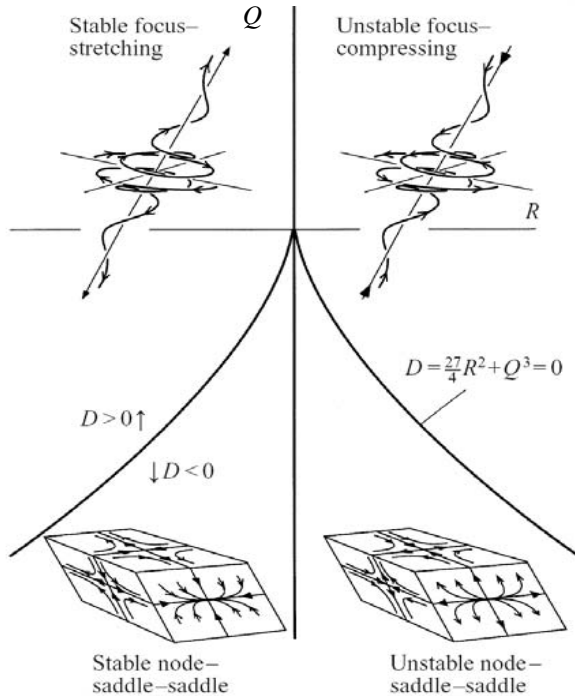


Reynolds Stress Associated with Incompressible Flow Patterns from the Q-R Invariants

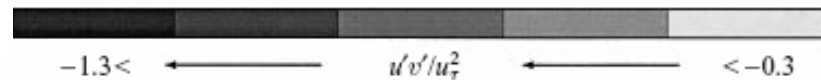
Grey levels show Reynolds shear stress amplitudes associated with Q-R incompressible flow patterns

Data from throughout $R_\theta = 670$ boundary layer DNS of Spalart

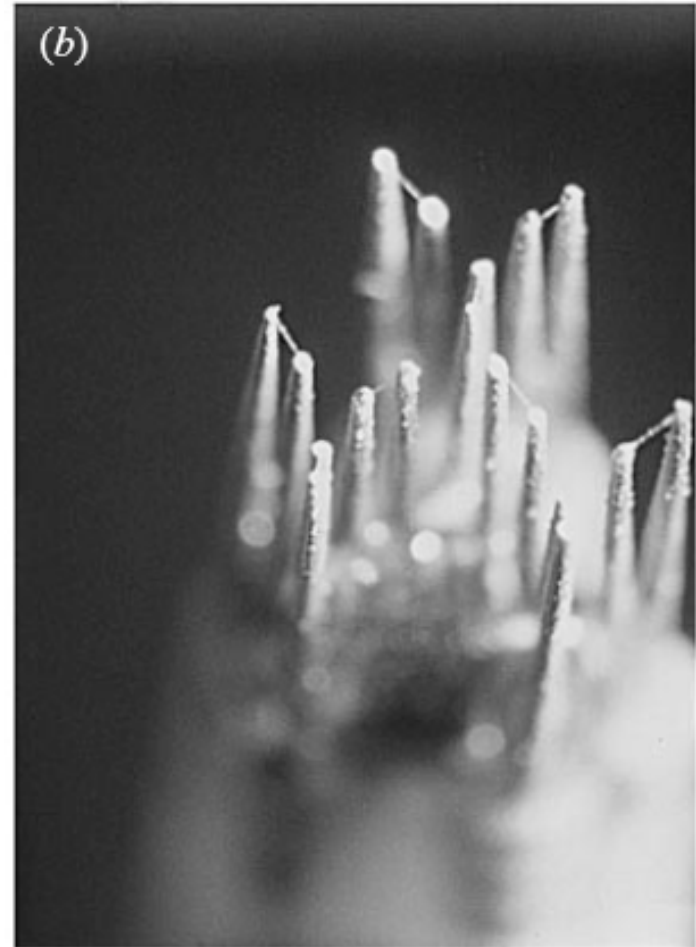
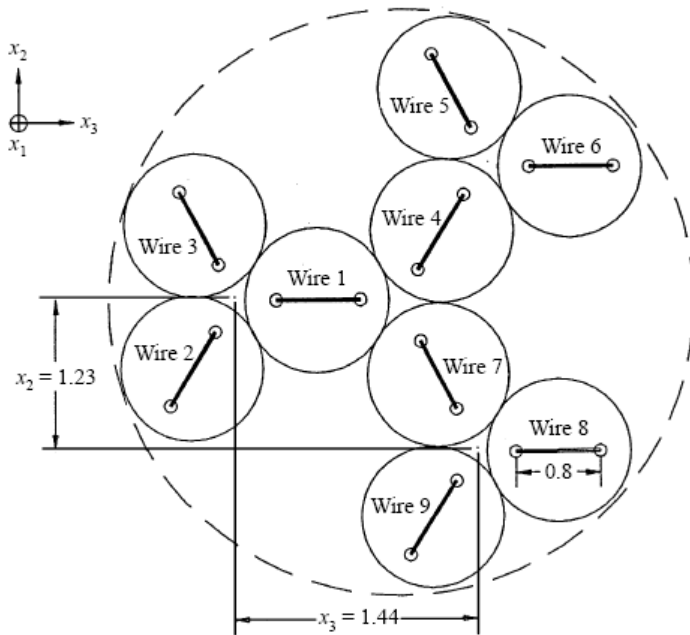
J.M. Chaćin & B. J. Cantwell (2000)
JFM 404



Sorted by quadrant decomposition



Nine-Sensor Hot-Wire Probe

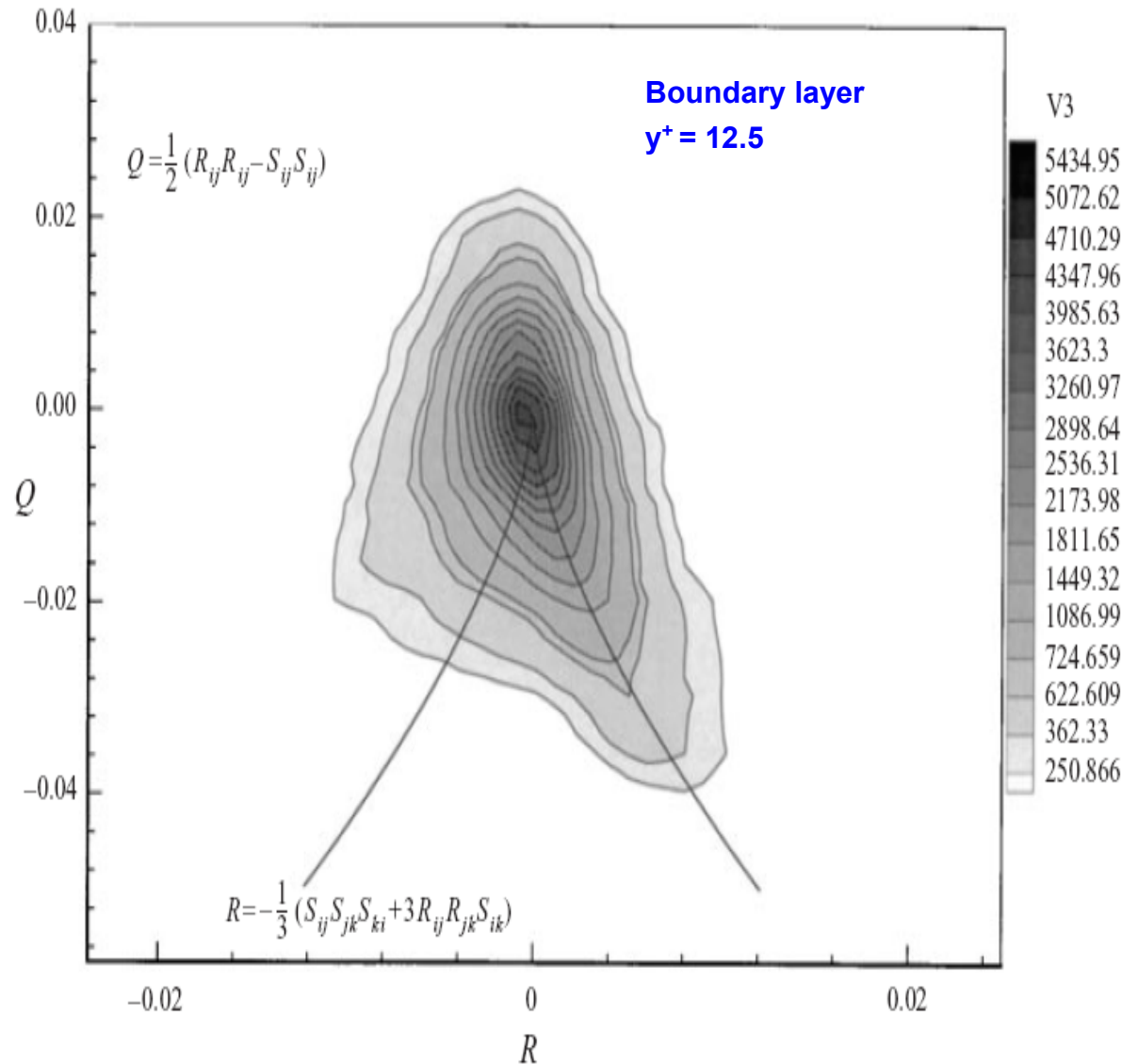


A. Honkan & Y. Andreopoulos (1997)
JFM 350

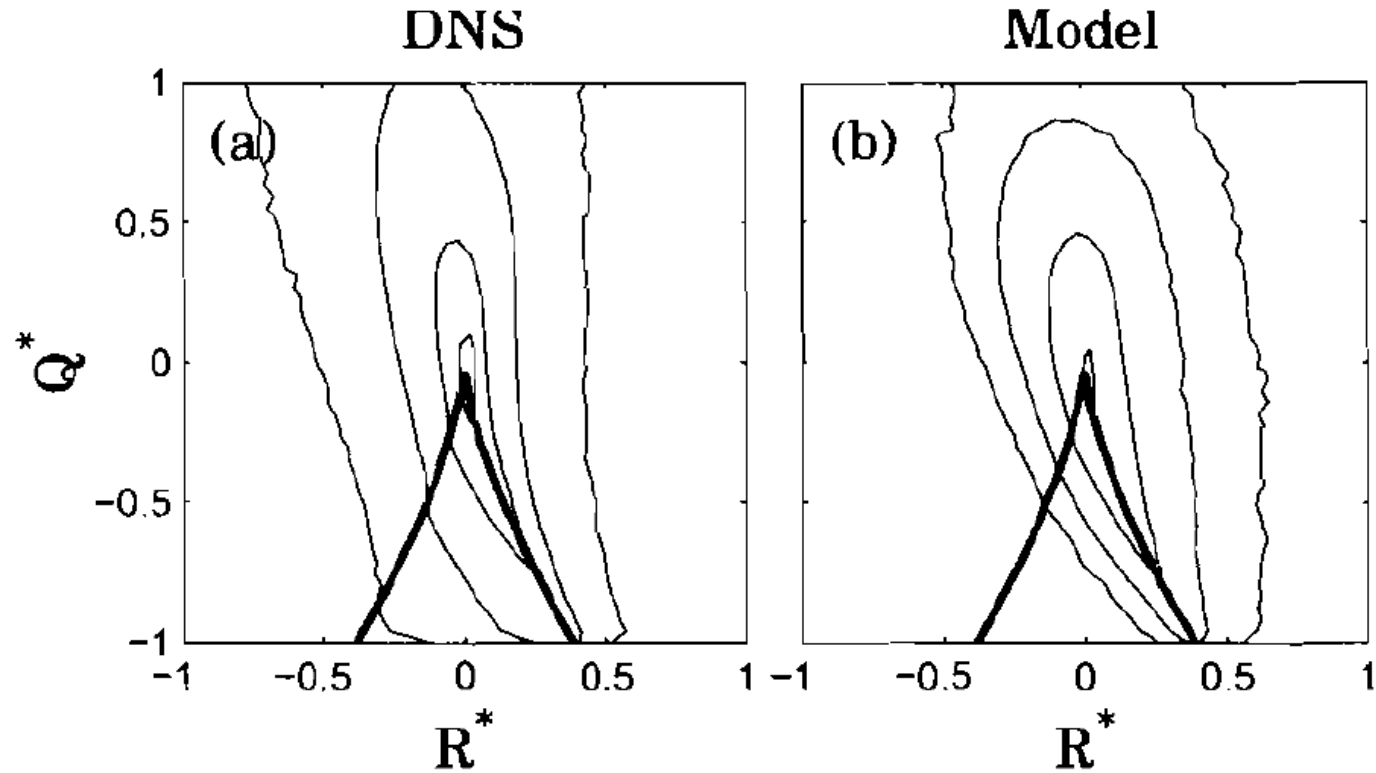
JPDF of the Q and R Invariants of the Velocity Gradient Tensor A_{ij}



Y. Andreopoulos & A. Honkan (2001)
JFM 439



JPDF of the Q and R Invariants of the Velocity Gradient Tensor A_{ij}



L. Chevillard, C. Meneveau, L. Biferale & F. Toschi (2008)
Phys. Fl. (to be published)

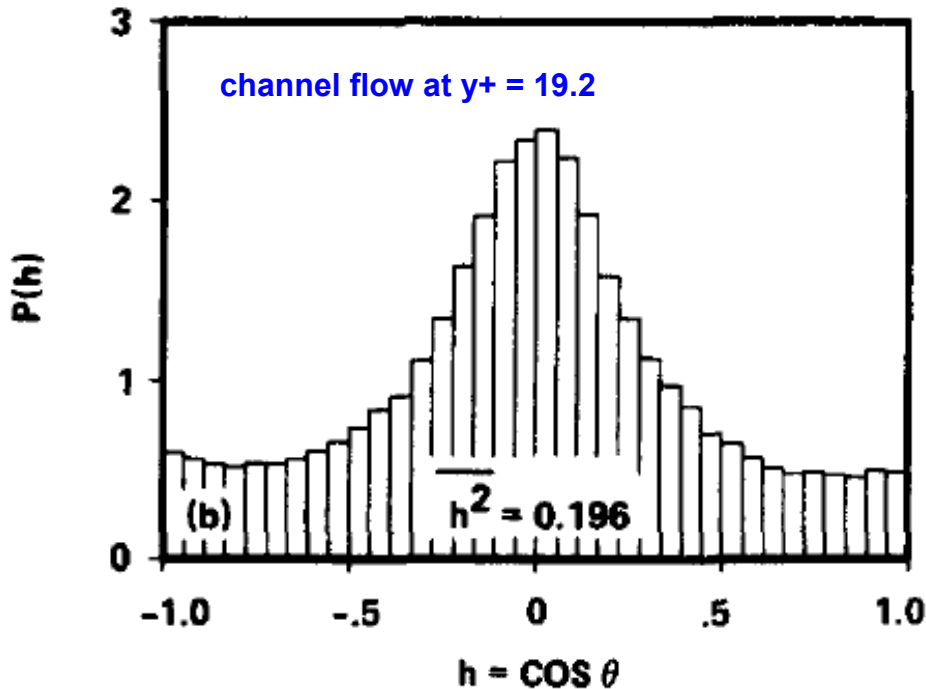


The Role of Helicity in Turbulence

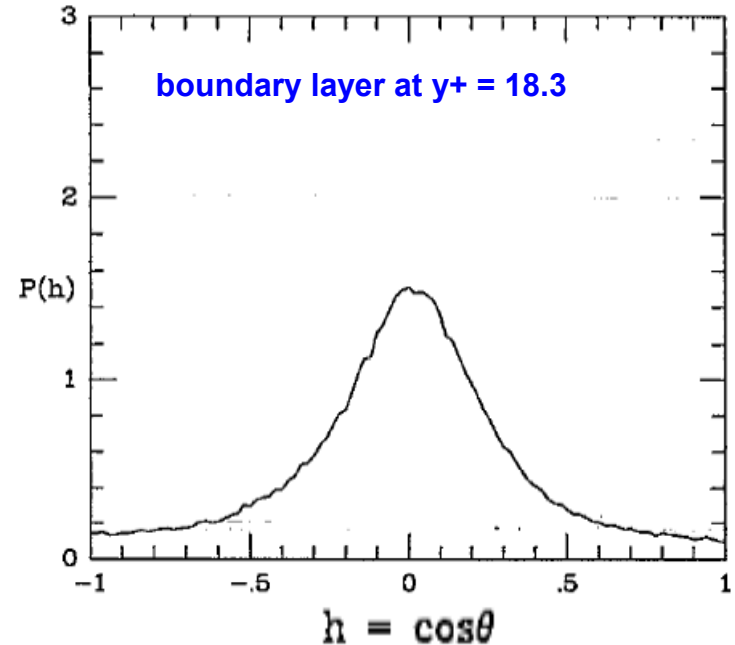
Moffat [(1985) *JFM* 159] speculated that turbulence might be described as steady solutions to the Euler equations about which unsteady solutions evolve. In the subdomains where the steady Euler solutions exist, the **relative helicity density**

$$h = (\mathbf{U} \cdot \boldsymbol{\Omega}) / |\mathbf{U}| |\boldsymbol{\Omega}| = \cos \theta$$

should be **maximal at ± 1** .



M. M. Rogers & P. Moin (1987)
Phys. Fl. 30

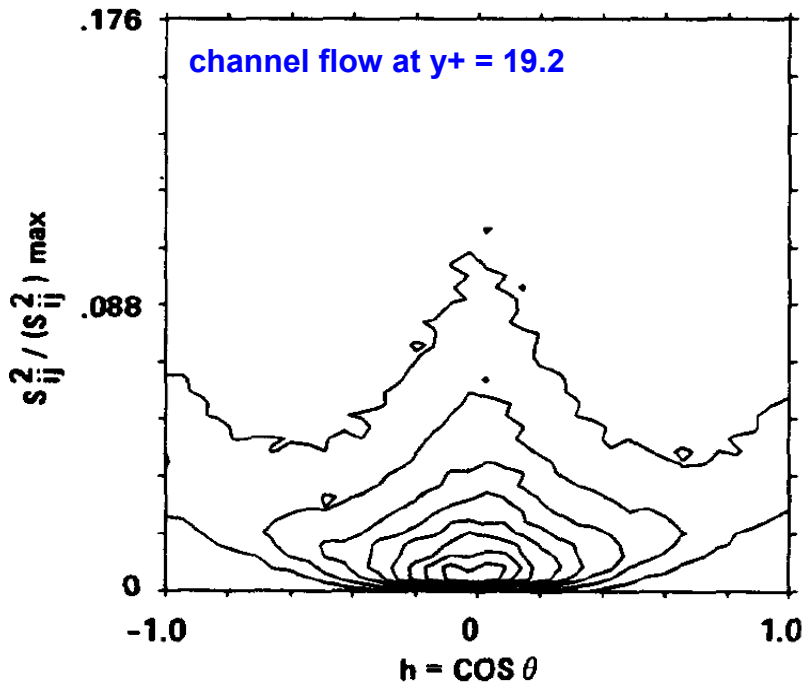


J.M. Wallace, J.-L. Balint & L. Ong (1992)
Phys. Fl. A 4

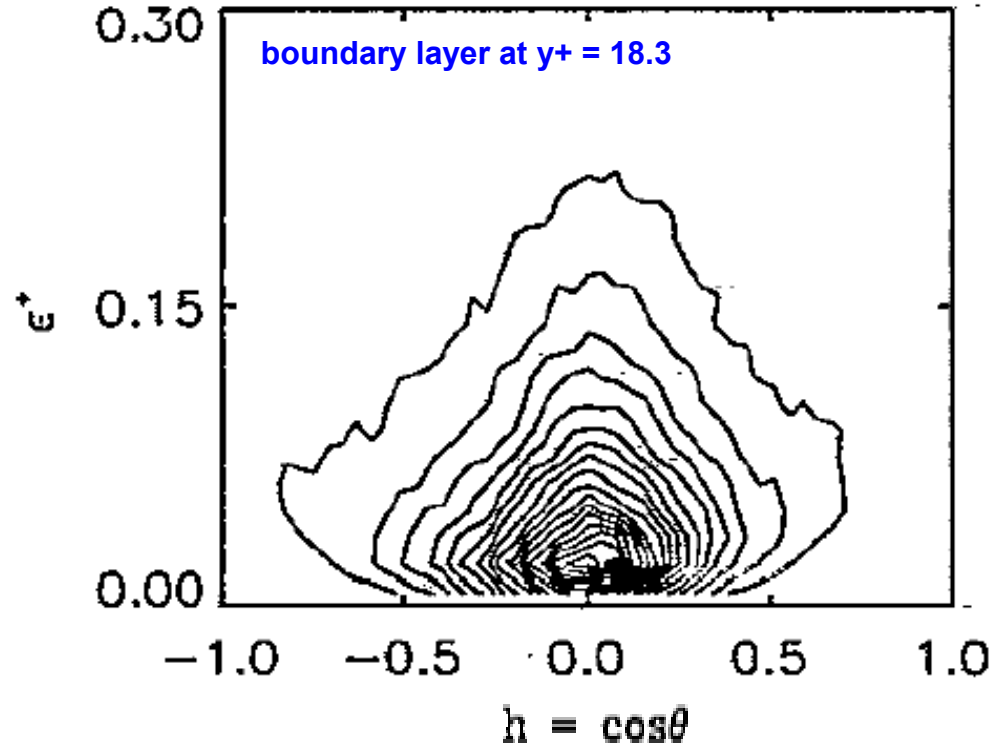


JPDFs of Relative Helicity Density and Dissipation Rate

Moffat further suggested that these subdomains could be considered to play the role of coherent structures in turbulence, and that the regions between these subdomains may be vortex sheets which should be the principal locus of viscous dissipation.



M. M. Rogers & P. Moin (1987)
Phys. Fl. 30



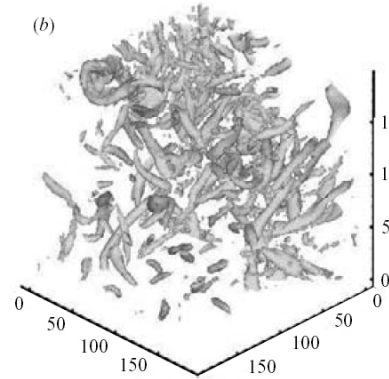
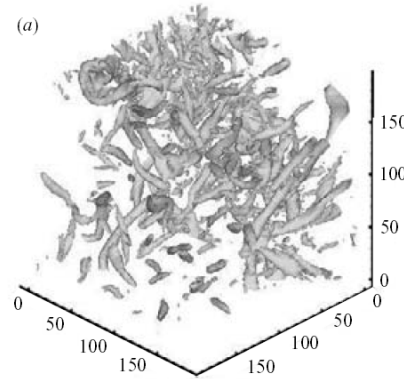
J.M. Wallace, J.-L. Balint & L. Ong (1992)
Phys. Fl. A 4

Low probability of large instantaneous dissipation rate and small (≈ 0) relative helicity density except in shear flow regions where ϵ amplitudes are small compared to the largest values in the flow domain



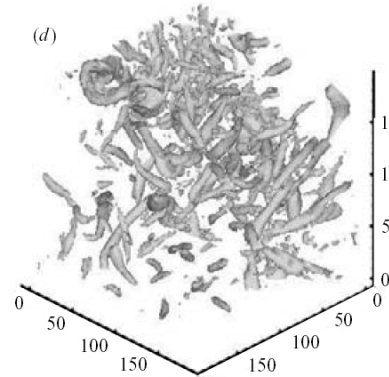
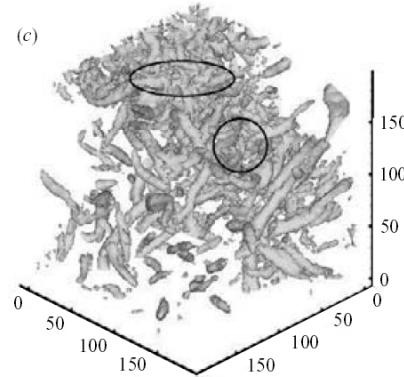
Schemes for Vortex Identification based on Velocity Gradient Tensor

λ_{ci} , Swirling strength, Zhou et al. (1999) JFM 387



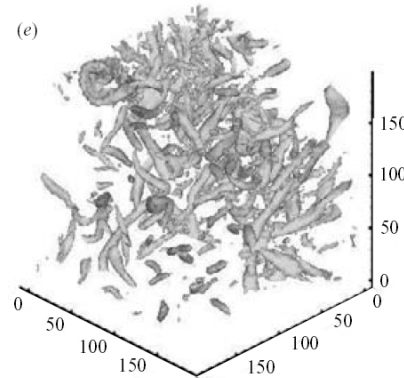
Q , Positive 2nd invariant, Hunt et al. (1988), CTR -S88

Δ , complex eigenvalues, Chong et al. (1990), Phys. Fluids A 2



λ_2 , local pressure minimum, Jeong & Hussain (1985), JFM 285

Λ_2 , special case



(f) $R_\lambda = 150$

Overlap volume	%
$\text{vol}(\lambda_{ci}, Q)/\text{vol}(\lambda_{ci})$	90.43
$\text{vol}(\lambda_{ci}, \Delta)/\text{vol}(\Delta)$	73.54
$\text{vol}(\lambda_{ci}, \lambda_2)/\text{vol}(\lambda_{ci})$	84.44
$\text{vol}(\lambda_{ci}, \lambda_2)/\text{vol}(\lambda_2)$	99.72
$\text{vol}(Q, \lambda_2)/\text{vol}(\lambda_2)$	98.65
$\text{vol}(Q, \lambda_2)/\text{vol}(Q)$	92.38
$\text{vol}(\lambda_2, \lambda_2)/\text{vol}(\lambda_2)$	99.58

P. Chakraborty, S. Balachandar & R. J. Adrian (2005), JFM 535



Animation of Vortex Structures in a Turbulent Boundary Layer



Evolution of Quasistreamwise Vortex Tubes and Wall Streaks in a Bubble-laden Turbulent Boundary Layer over a Flat Plate

A. Ferrante, S. Elghobashi, P. Adams, M. Valenciano, and D. Longmire

Physics of Fluids

**Vortex Identification with λ_2 ,
local pressure minimum,
Jeong & Hussain (1995), JFM
285**

http://pof.aip.org/pof/gallery/video/2004/901406phf_15MB.mov

Generation and Evolution of a Hairpin Vortices in a DNS Channel Flow



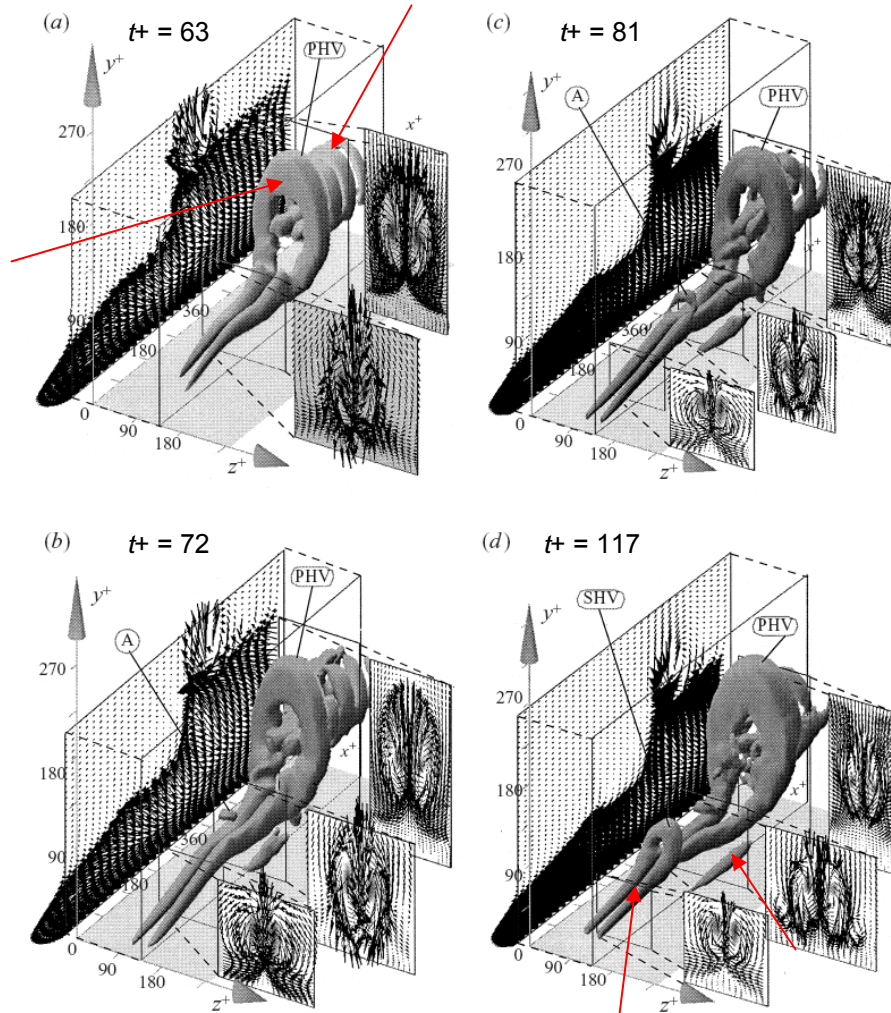
Primary vortex extracted from the two-point spatial correlation of the velocity field by linear stochastic estimation given a second-quadrant ejection event vector

New vortices are generated upstream of the primary vortex

They also are generated downstream and to the side of the primary vortex

These clusters of vortices are known as packets

J. ZHOU, R. J. ADRIAN, S. BALACHANDAR
& T. M. KENDALL (1999)
JFM 387



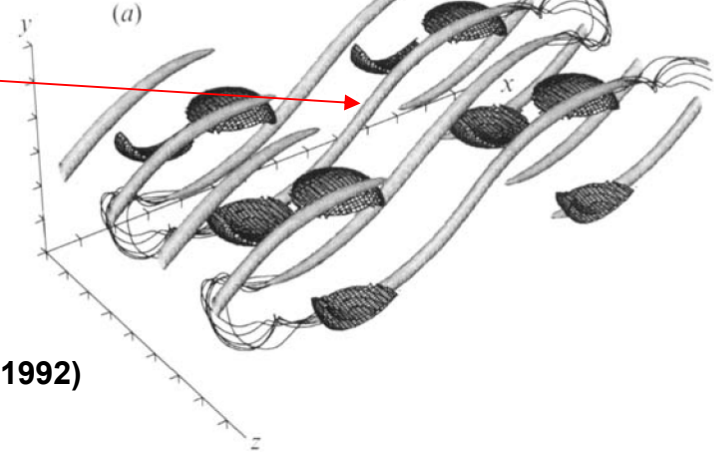


The Three-Dimensional Evolution of a Plane Mixing Layer: Kelvin–Helmholtz Rollup

Predominantly streamwise rib vortices develop in braid region between rollers.

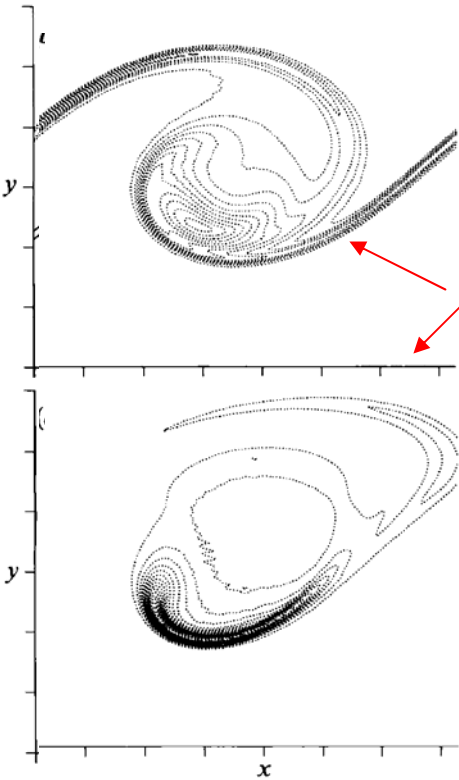
For certain initial conditions, persistent rib vortices do not develop. In such cases, the development of significant three-dimensionality is delayed.

Surfaces of constant vorticity magnitude

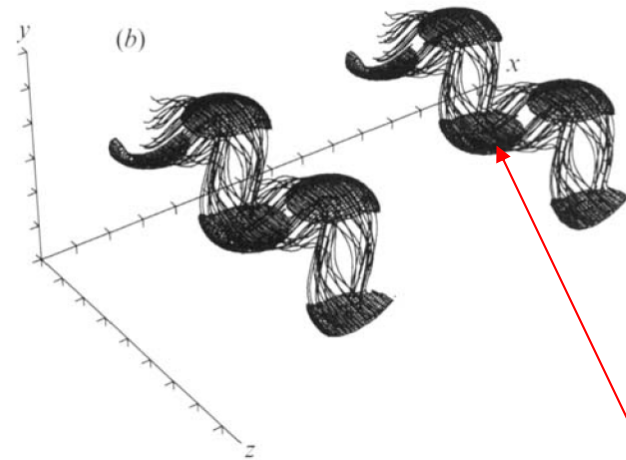


M. M. Rogers & R. D. Moser (1992)
JFM 243

Contours of ω_z indicating rollers in between ribs at two times. Solid positive. Dotted negative



vortex lines

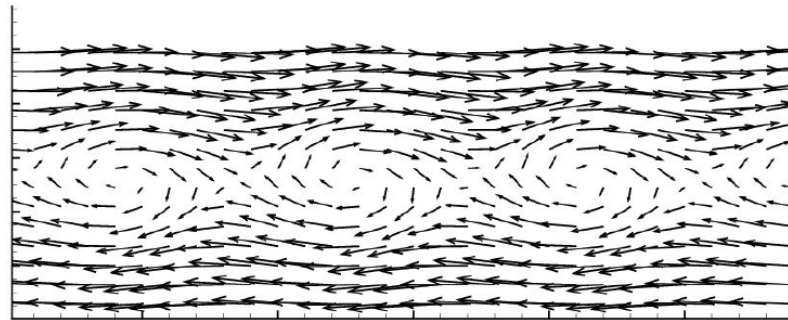


Spanwise vorticity rolls up into corrugated spanwise roller with vortex stretching creating strong spanwise vorticity in a **cup-shaped** region at the bends of the roller.



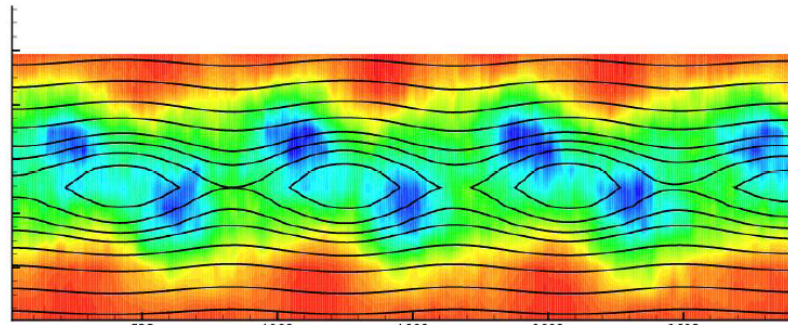
Spatial Relationship of Turbulent Production and Dissipation Rates to Roller Vortices in a Mixing Layer

Projection of **velocity vectors** on streamwise plane in a frame convecting with the mid-level velocity.



$U - U_c$

Phase averages constructed from single point measurements with 12-sensor probe and referenced to passage of roller vortices.

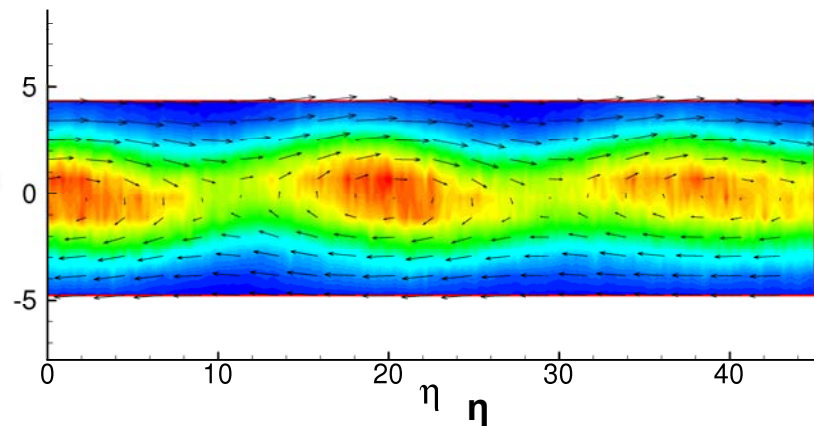


$\langle uv \rangle$

Reynolds shear stress (& production rate) conditionally phase averaged.

Dissipation rate conditionally phase averaged

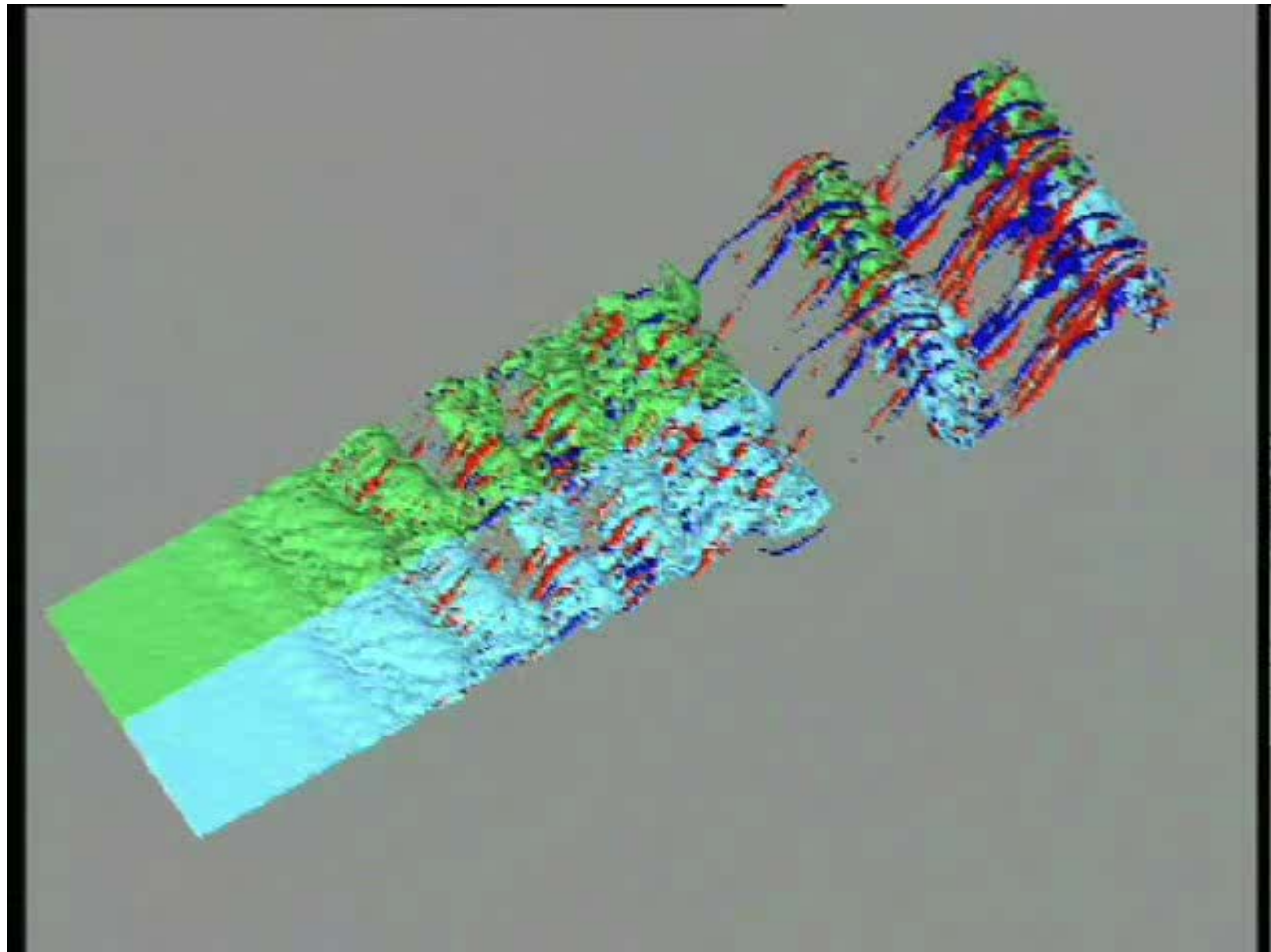
(b)



ϵ



Animation of Turbulent Mixing Layer LES



P. Comte, J. Silvestrini & P. Beégou
Eur. J. Mech B/Fluids 17 (1998)



Conclusions

Over the past **twenty years** remarkable **progress** has been made **in understanding** many aspects of the kinematics and dynamics of a wide variety of turbulent flows as a result of access to the **velocity gradient tensor**.

This progress is largely **due to technological developments** that have provided **experimental and computational tools** that were previously unavailable and to many clever people.

This great progress in understanding turbulence, in my view, shows that the oft stated idea that fluid mechanics is a “mature” field is far from true. **Our best days are ahead of us!**

Examples of this bright future are just up the road from me at Johns Hopkins in the **PIV** the **theoretical/DNS work of Charles Meneveau** (PRL 98, 2007) on the Lagrangian evolution of the velocity gradient tensor and the holographic PIV **work of Joe Katz shown at this meeting (paper AE3)**.